Performance analysis of a system with integrated CO_2 heat pumps and a PCM tank in different charging standards

Yantong Li[a], Natasa Nord[b], Chang Liu[a], Junhan Liang[a], Huibin Yin[a,*]

[a]Guangdong Provincial Key Laboratory of Distributed Energy Systems, Dongguan University of Technology, Dongguan 523808, China

[b]Department of Energy and Process Engineering, Norwegian University of Science and Technology, Trondheim NO-7491, Norway

[*]E-mail address: yinhb@dgut.edu.cn; phone: (+86) 0769-22861808

Abstract

Performance investigation of a system with an integrated heat pump and a phase change material (PCM) tank is seldom conducted in current studies, and the issue of identifying the optimal setting values of key variables in different charging standards and combinations of criteria is ignored. Therefore, in this study, we consider a system that integrates air- and water-source CO_2 heat pumps and a PCM tank as a case study to address this issue. Experimentally validated CO_2 heat pump and PCM tank models were used to simulate the system, and T-charging, Q-charging, and t-charging standards were considered. We concluded that the system coefficient of performance reduced by 10.5%, 12.2%, and 14.4% when the setting stored energy was increased from 2.1 kWh to 4.5 kWh, setting outlet water temperature of PCM tank was increased from 28 °C to 34 °C, and setting charging time was increased from 0.5 h to 1.7 h in the Q-charging, T-charging, and t-charging standards, respectively. Multicriteria optimization was performed in different cases to determine the optimal setting values of the key variables. The optimal setting charging time is 1.7 h when weight factors of charging time and stored energy are 0.3 and 0.7, respectively. Thus, this study provides a distinctive perspective for investigating a system by integrating a heat pump and PCM tank by considering different charging standards.

Keywords: CO_2 heat pump; PCM tank; Performance analysis; Charging standard

Nomenclature

E	Electricity use (kWh)
OS	Score (-)
Q	Energy amount (kWh)
T	Temperature (°C)
t	Moment (h)

Abbreviations

ACHP	Air-source CO_2 heat pump (-)
COP	Coefficient of performance (-)
PCM	Phase change material (-)
WCHP	Water-source CO_2 heat pump (-)

Subscripts

cp	Case considering ε_{ct} and COP_{st} (-)
cr	Compressor (-)
cs	Case considering ε_{ct} and Q_{se} (-)
cst	Case considering ε_{ct}, Q_{se}, and E_{tu} (-)
ct	Charging (-)
em	Ending (-)
lf	Least preferred case (-)
mf	Most preferred case (-)
ot	Outlet water of PCM tank (-)
pe	Pump at the evaporator side (-)
pg	Pump at the gas cooler side (-)
sm	Starting (-)
se	Stored (-)
st	System (-)
sv	Setting value (-)
tu	Total (-)

Greek symbols

α	Weigh factor (-)
ε	Time span (h)

1. Introduction

1.1. Background and motivation

Heat pumps that obtain heat from natural media, such as air [1] and water [2], are utilized in many fields, including household hot water utilization [3], drying [4], space heating [5], district heating [6] and cooling [7], waste heat recovery [8], rail transportation [9], and zero-emission vehicles [10]. CO_2, which is non-flammable, easy available, and environmentally friendly, is considered to be an ideal refrigerant in heat pumps. Owing to its transcritical refrigeration cycle, a CO_2 heat pump can produce high-temperature water [11]. Thermal energy storage improves the effectiveness and flexibility of energy utilization [12] and has been applied in many fields, including building envelopes [13], passive cooling [14], food supply chains [15], frozen products [16], thermal management [17], photovoltaic systems [18], hot water production [19], and solar stills [20]. PCM was added to the water tank to form a PCM tank with enhanced energy storage density. Thus, it is a significant component of heat-pump systems.

1.2. Research context

Wang et al. [21] investigated a heat pump system absorbing heat from the air and sun. They concluded that compared with the air-source heat pump system, the total electricity consumption (E_{tu}) could be reduced by 73.6%. Du et al. [22] also investigated a heat pump system absorbing heat from the air and sun. They found that the coefficient of performance (COP) of the system (COP_{st}) could reach 3.44. Shin et al. [23] performed a study of a water-source heat pump system. They found that the lifecycle cost of the system was 20.2% lower than that of the traditional system. Zhang et al. [24] reported that the COP of a solar-assisted heat pump was 50% higher than that of an air-source heat pump. Deng et al. [25] concluded that COP_{st} could be enhanced by 18.7% when a varying flowrate of heat transfer fluid at the evaporator side was applied in the ground-source heat pump system.

Ge et al. [26] concluded that the COP of a CO_2 heat pump with tube-in-tube heat exchanger could reach 4.47 when the ambient air temperature was 40 °C. Li et al. [27] conducted an investigation of a water-source CO_2 heat pump (WCHP) for domestic use. They found that the COP of the WCHP could reach 3.99 when the expansion valve opening was 28%. They also proposed a model-based sizing method that can identify the optimal gas cooler area to maximize the indicator,

considering the COP and cost. Sazon and Nikpey [28] reported that 5% increase in discharge pressure in a solar-assisted ground-source CO_2 heat pump could contribute to 5% reduction in the levelized cost of heating. Duarte et al. [29] found that increasing the inlet water temperature at the gas cooler side from 15 °C to 35 °C would cause the COP of the solar-assisted CO_2 heat pump to decrease by 45.8%. Zanetti et al. [30] found that electricity production can be increased by 8% when a photovoltaic-thermal solar collector was combined with a CO_2 heat pump.

Huang et al. [31] experimentally investigated the performance of a solar chimney with phase change material (PCM). They found that the PCM melting time was 13.3% longer when the inclination angle was 30° than that when it was 60°. Guermat et al. [32] concluded that the indoor temperature could be reduced by 3.95 °C when PCM was applied in the building envelope. Khan et al. [33] found that the output power could be enhanced by 9.69% when PCM was utilized in a photovoltaic system. Maghrabie et al. [34] concluded that the output power could be increased by 15.8% when a 3 cm thick PCM panel was utilized in a photovoltaic system. Zheng et al. [35] reported that E_{tu} of a solar heating system could be reduced by 35.7% when the PCM floor was used.

Qv et al. [36] concluded that the COP of a solar-assisted heat pump with a PCM tank was 65% higher than that of an air-source heat pump. Zou et al. [37] reported that the energy storage density increased by 14% when the PCM tank was utilized in a heat pump system. Long and Zhu [38] concluded that the COP of a system integrating a heat pump and PCM tank could reach 3.08. Moreno et al. [39] found that additional cooling of 14.5% could be supplied when the PCM tank was applied to a heat pump system for space cooling purposes. Qiu et al. [40] concluded that the charging time (ε_{ct}) of the PCM tank could be reduced by 29.8% when the nanoparticle and orthogonal fin were applied. Issa and Thirunavukkarasu [41] found that the storage efficiency could reach 82% when copper cylindrical capsules were utilized in the PCM tank. Peng et al. [42] reported that the charging rate of the PCM tank can be increased by 20% when fins are applied. Shu et al. [43] found that ε_{ct} of the PCM tank could be reduced by 56% when the temperature was increased from 65 °C to 85 °C.

Although scholars have paid attention to investigating heat pump systems with PCM tanks, few

studies have systematically focused on the performance of the charging process with the integration of the heat pump and PCM tank. When the PCM tank was integrated with the heat pump, the increase in the outlet water temperature of the PCM tank (T_{ot}) slowed owing to the phase-change process. This contributes to the enhancement of energy efficiency. However, scholars have ignored this issue. The charging process of PCM in this study was open-loop. ε_{ct}, stored energy (Q_{se}), and T_{ot} were considered as performance indicators. However, the charging process with the integration of the PCM tank and heat pump was a closed loop. E_{tu} and COP_{st} were considered as performance indicators.

As depicted in Table 1, unlike current studies, this work focuses on investigating the charging process at system level, and ε_{ct}, Q_{se}, E_{tu}, and COP_{st} are considered as performance indicators. The knowledge gaps for investigating the system integrating CO_2 heat pumps with a PCM tank are as follows. a) The performance investigation of the system in different charging standards is seldom considered in current studies; b) The systematic investigation of different setting variables in different charging standards on ε_{ct}, Q_{se}, E_{tu}, and COP_{st} is still lacking; c) The approach for identifying optimal setting variables in different charging standards to maximize the overall performance of the system requires much-needed development; d) The influence mechanism of different combinations of setting variables on the performance of the system is still unknown.

Table 1 Comparison between current studies and this work

References	System level	Component level	Charging process	ε_{ct}	Q_{se}	E_{tu}	COP_{st}
[36]	√	×	×	×	×	×	√
[37]	√	×	×	×	×	×	√
[38]	√	×	×	×	×	×	√
[39]	√	×	×	√	√	×	×
[40]	×	√	√	√	×	×	×
[41]	√	×	√	√	√	×	×
[42]	×	√	√	√	×	×	×
[43]	×	√	√	√	×	×	×
This work	√	×	√	√	√	√	√

1.3. Contributions

The contributions or novelties of this study are as follows. a) The influence of different charging standards on the performance of the system integrating CO_2 heat pumps with PCM tank was analyzed. This remedies the research gap in the field of system integration in different charging standards; b) The influence of $Q_{se,sv}$ in the Q-charging standard, $T_{ot,sv}$ in the T-charging standard, and $\varepsilon_{ct,sv}$ in the t-charging standard on ε_{ct}, Q_{se}, E_{tu}, and COP_{st} were analyzed. This overcomes the limitations in current studies that the influencing factor in the aspects of integrating the PCM tank with CO_2 heat pumps is simple; c) A multi-criteria approach was established to identify optimal $Q_{se,sv}$, $T_{ot,sv}$, and $\varepsilon_{ct,sv}$ in the Q-charging, T-charging, and t-charging standards, respectively. Unlike current studies, this study can guide engineers to design optimal systems integrating CO_2 heat pumps with a PCM tank in different charging standards; d) Three multi-criteria cases in which the combinations of ε_{ct} and Q_{se}, combinations of ε_{ct}, E_{tu}, and Q_{se}, and combinations of ε_{ct} and COP_{st} were considered to enable better operation of the system integrating CO_2 heat pumps with a PCM tank in different aspects.

1.4. Paper organization

The remainder of this paper is organized as follows. In Section 2, the material and methods of this study are presented. The description of the case study is presented in Section 3. In Section 4, we present the results and analysis in different charging standards. The conclusions are presented in Section 5. Finally, in Section 6, we present the future prospects.

2. Material and methods

The influence of charging standards, i.e., how to judge whether the charging process is completed, on the performance of the system has seldom been considered in current studies. In this study, T_{ot} was monitored using a temperature sensor. The charging process is considered complete when T_{ot} reaches the setting value of T_{ot} ($T_{ot,sv}$). This charging standard is known as the T-charging standard. However, limited thermal energy is sometimes required from the PCM tanks. In this study, Q_{se} was monitored using an energy meter. The charging process is considered complete when Q_{se} reaches the setting value of Q_{se} ($Q_{se,sv}$). This charging standard is known as the Q-charging standard. In the other cases, the time required to charge the PCM tank was limited. The charging process is considered as being completed when ε_{ct} reaches the setting value of ε_{ct} ($\varepsilon_{ct,sv}$). This

charging standard is known as the t-charging standard. The final two charging standards are not considered in current studies. Additionally, the influence of combinations of setting variables on the system performance is unclear.

Overall, a systematic investigation of the charging process with the integration of a heat pump and PCM tank considering different charging standards and combinations of setting variables is lacking. Therefore, in this study, we considered a charging process with the integration of CO_2 heat pumps and a PCM tank as a case study to illustrate the influence of the charging standards and combinations of setting variables on the performance of the system. An air-source CO_2 heat pump (ACHP) and WCHP were considered. The experimentally validated CO_2 heat pump and PCM tank models were used to simulate the charging process. T-charging, Q-charging, and t-charging standards were considered. Additionally, three multi-criteria cases, which included the combinations of ε_{ct} and Q_{se}, ε_{ct}, E_{tu}, and Q_{se}, and ε_{ct} and COP_{st}, were considered. Through multi-criteria optimization, optimal $T_{ot,sv}$, $Q_{se,sv}$, and $\varepsilon_{ct,sv}$ were determined in the T-charging, Q-charging, and t-charging standards, respectively.

Fig. 1 illustrates the research methodology. The main parts of this study include the establishment of the simulation platform, results, and analyses. Part of the simulation platform is composed of an understanding of the physical characteristics, development of mathematical models, and definition of performance indexes. To understand the physical characteristics of the system integrating the CO_2 heat pumps and PCM tank, the components and operating principles of the system were determined. The main mathematical models of the system included the CO_2 heat pump and PCM tank models. In the CO_2 heat pump model, an evaporator, liquid receiver, internal heat exchanger, compressor, and gas cooler were considered. The performance indices were defined by considering time and energy. Multiple criteria have been proposed to evaluate the performance of the system. Three charging standards: Q-charging, T-charging, and t-charging, were considered in the results and analyses. For each charging standard, the influence of setting variables on ε_{ct}, E_{tu}, Q_{se}, and COP_{st} were analyzed. Different combinations of setting variables and weight factors were considered in the multi-criteria optimization, and the optimal setting variables in each case were obtained.

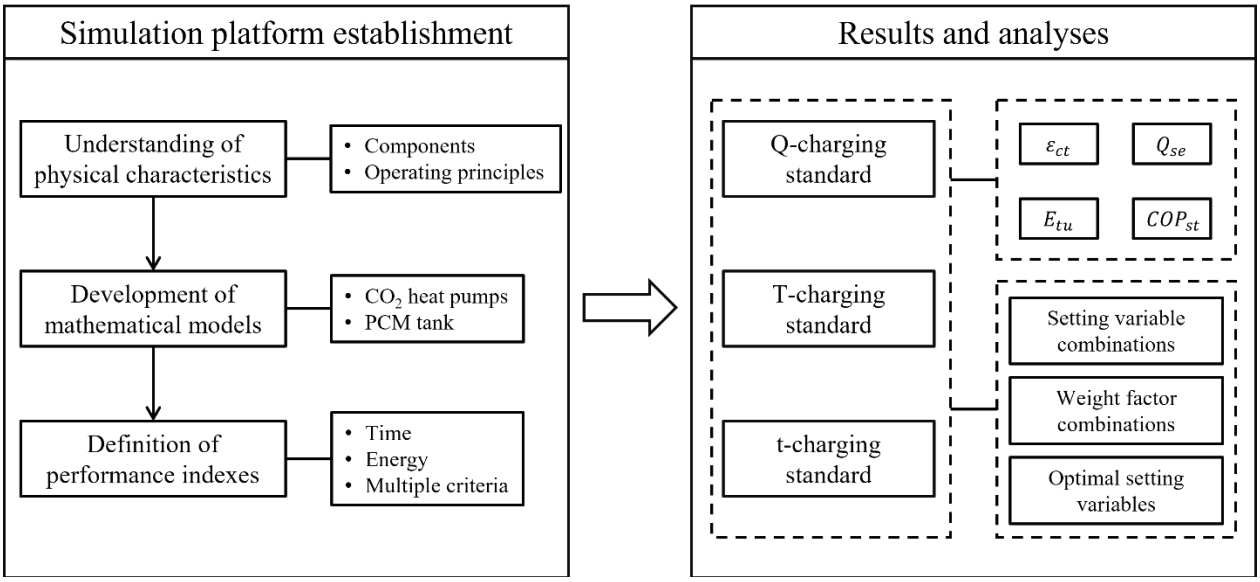

Fig. 1. Research methodology of this study

2.1. Understanding of physical characteristics

Fig. 2 shows a diagram of the system with the integration of CO_2 heat pumps and a PCM tank. ACHP and WCHP systems were considered. Valve-1 and valve-2 were utilized to realize the switch between the ACHP and WCHP. The gas cooler, compressor, evaporator, expansion valve, and liquid receiver are the main components of the CO_2 heat pumps. Water and air provided heat for the CO_2, which was throttled and compressed in the expansion valve and compressor, respectively. CO_2 evaporates in the evaporator. The internal heat exchanger increases the CO_2 temperature at the compressor inlet by acquiring heat from the CO_2 leaving the gas cooler. The water in the PCM tank was heated from the gas cooler by driving the pump.

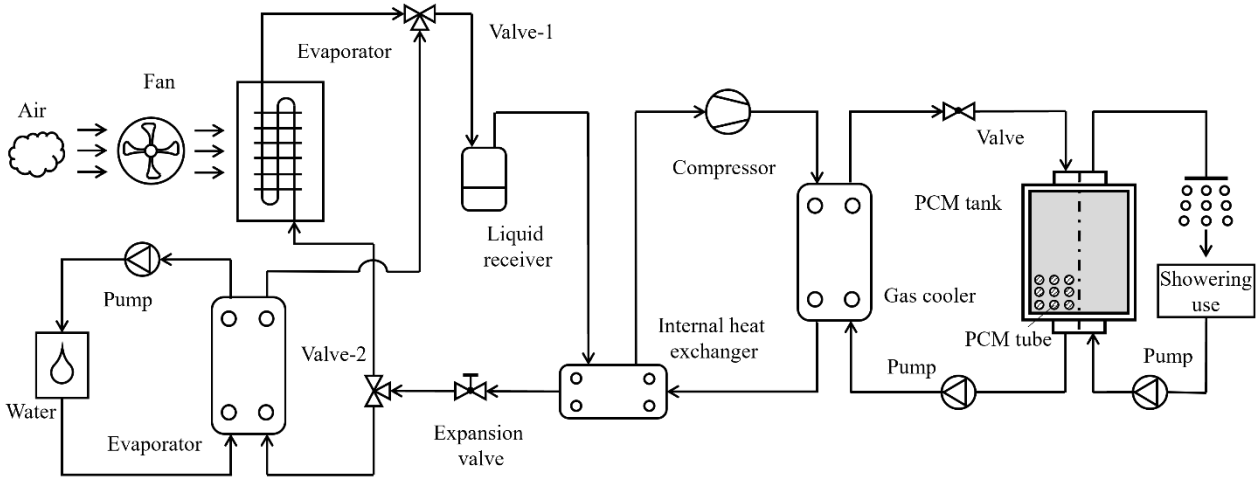

Fig. 2. Diagram of the system with integrated CO_2 heat pumps and a PCM tank for household use

2.2. Development of mathematical models

The system was simulated by integrating the CO_2 heat pump and PCM tank models. The assumptions for constructing the CO_2 heat pump and PCM tank models were presented by Rasmussen et al. [44] and Li et al. [45], respectively. The formulas for calculating the heat transfer coefficients of the heat exchangers in the CO_2 heat pump model are described in studies of Deng et al. [46], Lee et al. [47], and Mota et al. [48]. The formulas for the compressor and expansion valve models are presented in the studies of Wang et al. [49] and Eames et al. [50], respectively. The formulas for calculating the Nusselt number in the PCM tank model were presented by Watanabe et al. [51]. Validations of CO_2 heat pump and PCM tank models were presented by Li et al. [2]. The mean difference between simulated and experimental outlet water temperatures on the gas cooler side was 1.4 K, and the error of the PCM tank model was 3.97%, which proves the reliability of these models.

2.3. Definition of performance indexes

ε_{ct}, Q_{se}, E_{tu}, and COP_{st} were utilized as performance indexes. ε_{ct} is calculated using Eq. (1) [52]:

$$\varepsilon_{ct} = t_{em} - t_{sm} \tag{1}$$

where t_{em} and t_{sm} denote the ending and starting moments, respectively. E_{tu} was calculated using Eq. (2) [53]:

$$E_{tu} = E_{cr} + E_{pe} + E_{pg} \tag{2}$$

where E_{cr}, E_{pe}, and E_{pg} are the electricity used by the compressor, and pumps at the evaporator and gas cooler sides, respectively. COP_{st} was calculated using Eq. (3) [2]:

$$COP_{st} = \frac{Q_{se}}{E_{tu}} \tag{3}$$

3. Case study

The water source evaporator, which has a plate width of 0.101 m, has 40 plates. The air-source evaporator has a fin thickness, spacing, and height of 0.24 mm, 5 mm, and 3.5 mm, respectively. The heat transfer fluid was a mixture of water and propylene glycol in the ratio of 70:30. The gas cooler, which had a plate width of 0.1195 m, had 30 plates. The internal heat exchanger had a plate width of 0.076 m and 12 plates. The PCM used in this study was paraffin. The melting temperature, thermal conductivity, latent heat, density, and solid and liquid specific heat were 18 °C, 0.17 W/(m·K), 236 kJ/kg, 780 kg/m^3, 1.65 kJ/(kg·K) and 2.1 kJ/(kg·K), respectively [2].

A multicriteria method was used to determine the optimal setting values for different charging standards [54]. In the Q-charging, T-charging, and t-charging standards, $Q_{se,sv}$, $T_{ot,sv}$, and $\varepsilon_{ct,sv}$ were considered as optimization variables, respectively. The aim of optimization was to maximize the overall performance score by identifying the optimal setting values. Three cases were considered when the multi-criteria method was used. In the first case, ε_{ct} and Q_{se} were considered. The overall performance score in this case (OS_{cs}) was calculated using Eq. (4):

$$OS_{cs} = \alpha_{\varepsilon_{ct}} \cdot OS_{\varepsilon_{ct}} + \alpha_{Q_{se}} \cdot OS_{Q_{se}} \quad (4)$$

where $\alpha_{\varepsilon_{ct}}$ and $\alpha_{Q_{se}}$ are user-specified weight factors. Note that the sum of $\alpha_{\varepsilon_{ct}}$ and $\alpha_{Q_{se}}$ is 1. In the second case, ε_{ct}, Q_{se}, and E_{tu} were considered. The overall performance score (OS_{cst}) was calculated using Eq. (5):

$$OS_{cst} = \alpha_{\varepsilon_{ct}} \cdot OS_{\varepsilon_{ct}} + \alpha_{Q_{se}} \cdot OS_{Q_{se}} + \alpha_{E_{tu}} \cdot OS_{E_{tu}} \quad (5)$$

where $\alpha_{E_{tu}}$ is the user-specified weight factor. Note that the sum of $\alpha_{\varepsilon_{ct}}$, $\alpha_{Q_{se}}$, and $\alpha_{E_{tu}}$ is 1. In the third case, ε_{ct} and COP_{st} were considered. The overall performance score (OS_{cp}) was calculated using Eq. (6):

$$OS_{cp} = \alpha_{\varepsilon_{ct}} \cdot OS_{\varepsilon_{ct}} + \alpha_{COP_{st}} \cdot OS_{COP_{st}} \quad (6)$$

where $\alpha_{COP_{st}}$ is the user-specified weight factor. Note that the sum of $\alpha_{\varepsilon_{ct}}$ and $\alpha_{COP_{st}}$ is 1. For the formulas for calculating the overall performance score in different cases, i.e., Eqs. (4)–(6), refer to the studies of Li et al. [2, 54]. In [2], the formula for calculating the overall performance score was the same as Eq. (6). In [54], the formula for calculating the overall performance score considered the initial cost, total electricity use (E_{tu}), thermal discomfort ratio, and operating cost.

$OS_{\varepsilon_{ct}}$, $OS_{Q_{se}}$, $OS_{E_{tu}}$, and $OS_{COP_{st}}$ are respectively determined using Eqs. (7)–(10):

$$OS_{\varepsilon_{ct}} = \frac{\varepsilon_{ct} - \varepsilon_{ct,lf}}{\varepsilon_{ct,mf} - \varepsilon_{ct,lf}} \quad (7)$$

$$OS_{Q_{se}} = \frac{Q_{se} - Q_{se,lf}}{Q_{se,mf} - Q_{se,lf}} \quad (8)$$

$$OS_{E_{tu}} = \frac{E_{tu} - E_{tu,lf}}{E_{tu,mf} - E_{tu,lf}} \quad (9)$$

$$OS_{COP_{st}} = \frac{COP_{st} - COP_{st,lf}}{COP_{st,mf} - COP_{st,lf}} \quad (10)$$

where lf and mf represent the least and most preferred circumstances, respectively. For the formulas for calculating $OS_{\varepsilon_{ct}}$, $OS_{Q_{se}}$, $OS_{E_{tu}}$, and $OS_{COP_{st}}$, i.e., Eqs. (7)–(10), which are normalized

as ε_{ct}, Q_{se}, E_{tu}, and COP_{st}, respectively, refer to the studies of Li et al. [2, 54]. In [2], ε_{ct} and COP_{st} are normalized. In [54], the initial cost, E_{tu}, thermal discomfort ratio, and operating cost were normalized.

4. Results and discussion

This section presents the results and discussion in Q-charging, T-charging, and t-charging standards. $Q_{se,sv}$, $T_{ot,sv}$, and $\varepsilon_{ct,sv}$ are considered as decision variables in Q-charging, T-charging, and t-charging standards, respectively. ε_{ct}, Q_{se}, E_{tu}, and COP_{st} are considered as performance indicators.

4.1. Results and discussion in the Q-charging standard

In this section, we analyze the effects of $Q_{se,sv}$ on ε_{ct}, Q_{se}, E_{tu}, and COP_{st} in the Q-charging standard. Fig. 3 depicts the variations of ε_{ct}, Q_{se}, E_{tu}, and COP_{st} with $Q_{se,sv}$ when ACHP is utilized. In Fig. 3(a), ε_{ct} linearly increased with the increase in $Q_{se,sv}$. This implies that more time is required to complete the charging process to satisfy higher energy demands. As shown in Fig. 3(b), Q_{se} increased linearly with an increase in $Q_{se,sv}$. The Q_{se} values were almost identical to those of $Q_{se,sv}$, indicating that the Q-charging standard was successfully achieved. As shown in Fig. 3(c), E_{tu} increases linearly with $Q_{se,sv}$. This means that more electricity is required to satisfy higher energy demands. As shown in Fig. 3(d), COP_{st} reduced as $Q_{se,sv}$ increased. According to Eq. (3), this phenomenon implies that the degree of increase in Q_{se} with $Q_{se,sv}$ is smaller than that of E_{tu} with $Q_{se,sv}$. For instance, Q_{se} was 2.1 kWh and 2.5 kWh when $Q_{se,sv}$ was 2.1 kWh and 2.5 kWh, respectively. E_{tu} was 0.7 kWh and 0.86 kWh when $Q_{se,sv}$ was 2.1 kWh and 2.5 kWh, respectively. Thus, when $Q_{se,sv}$ increased from 2.1 kWh to 2.5 kWh, Q_{se} and E_{tu} increased by 19% and 22.8%, respectively. This indicates that the increasing degree of Q_{se} with $Q_{se,sv}$ is smaller than that of E_{tu} with $Q_{se,sv}$. According to Eq. (3), COP_{st} was 3 and 2.92 when $Q_{se,sv}$ was 2.1 kWh and 2.5 kWh, respectively. Thus, the phenomenon of the increasing degree of Q_{se} with $Q_{se,sv}$ was smaller than that of E_{tu} with $Q_{se,sv}$ caused that COP_{st} reduced as $Q_{se,sv}$ increased.

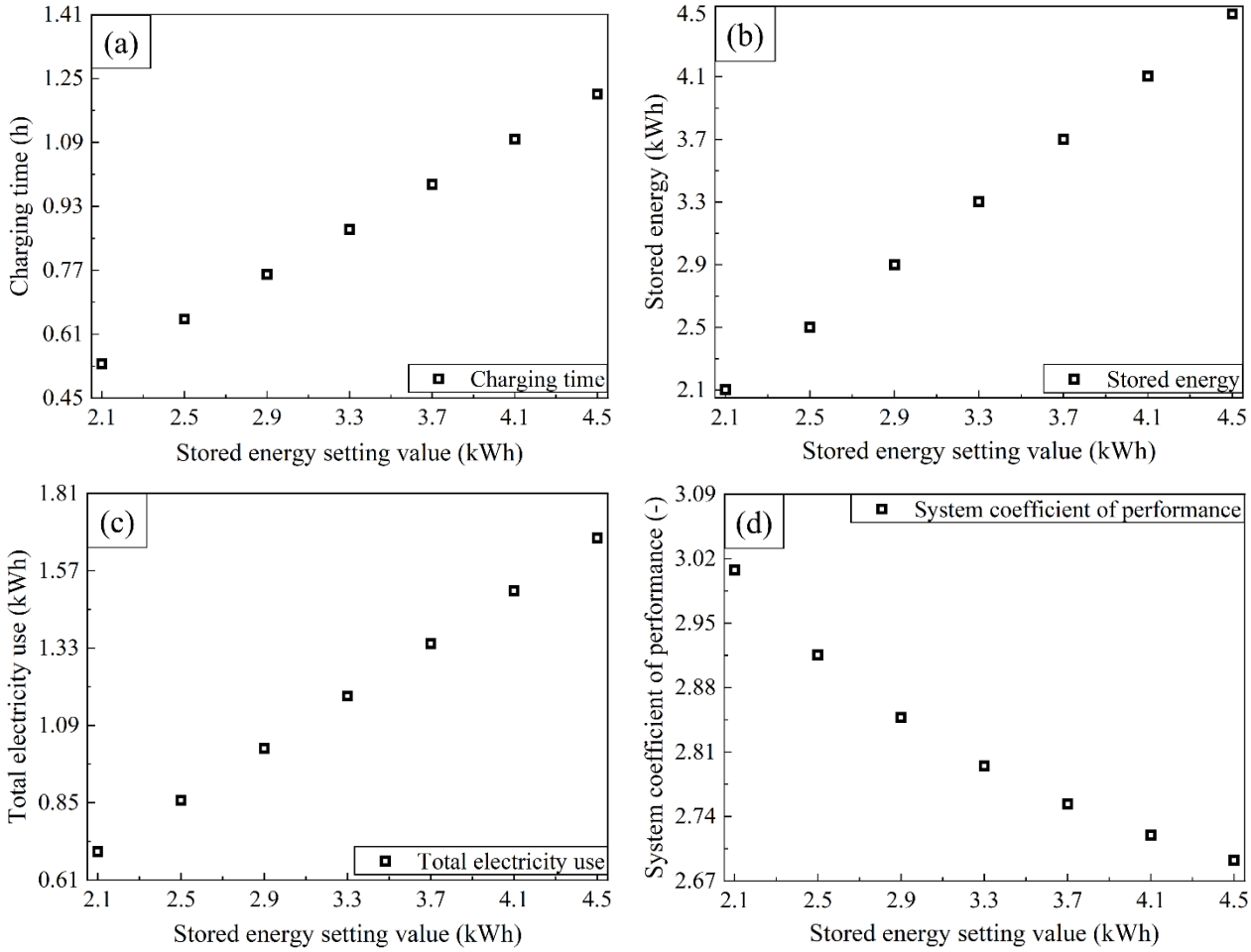

Fig. 3. (a) ε_{ct}, (b) Q_{se}, (c) E_{tu}, and (d) COP_{st} in different $Q_{se,sv}$ when ACHP is utilized

Fig. 4 depicts the variations in OS_{cs}, OS_{cst}, and OS_{cp} with $Q_{se,sv}$ when ACHP is utilized. In Fig. 4(a), the optimal $Q_{se,sv}$ were 4.5 kWh and 2.1 kWh in situations when $\alpha_{\varepsilon_{ct}}$: $\alpha_{Q_{se}}$ were 0.3:0.7 and 0.7:0.3, respectively. When $\alpha_{\varepsilon_{ct}}$: $\alpha_{Q_{se}}$ was 0.5:0.5, the variation of OS_{cs} with $Q_{se,sv}$ was small; the optimal $Q_{se,sv}$ was 3.3 kWh. Thus, the larger $\alpha_{\varepsilon_{ct}}$ would cause the optimal $Q_{se,sv}$ to occur at a smaller value. In Fig. 4(b), the optimal $Q_{se,sv}$ was 2.1 kWh when $\alpha_{\varepsilon_{ct}}$: $\alpha_{Q_{se}}$: $\alpha_{E_{tu}}$ were 0.2:0.3:0.5 and 0.3:0.4:0.3. When $\alpha_{\varepsilon_{ct}}$: $\alpha_{Q_{se}}$: $\alpha_{E_{tu}}$ was 0.2:0.5:0.3, the variation of OS_{cst} with $Q_{se,sv}$ was small; the optimal $Q_{se,sv}$ was 3.3 kWh. Thus, it seemed that the smaller $\alpha_{Q_{se}}$ would cause the optimal $Q_{se,sv}$ to occur at the smaller value. In Fig. 4(c), the optimal $Q_{se,sv}$ is 2.1 kWh irrespective of $\alpha_{\varepsilon_{ct}}$: $\alpha_{COP_{st}}$ being 0.3:0.7, 0.5:0.5, or 0.7:0.3. Thus, regardless of whether ε_{ct} had a larger or smaller weighting than COP_{st}, the optimal $Q_{se,sv}$ occurred at a smaller value.

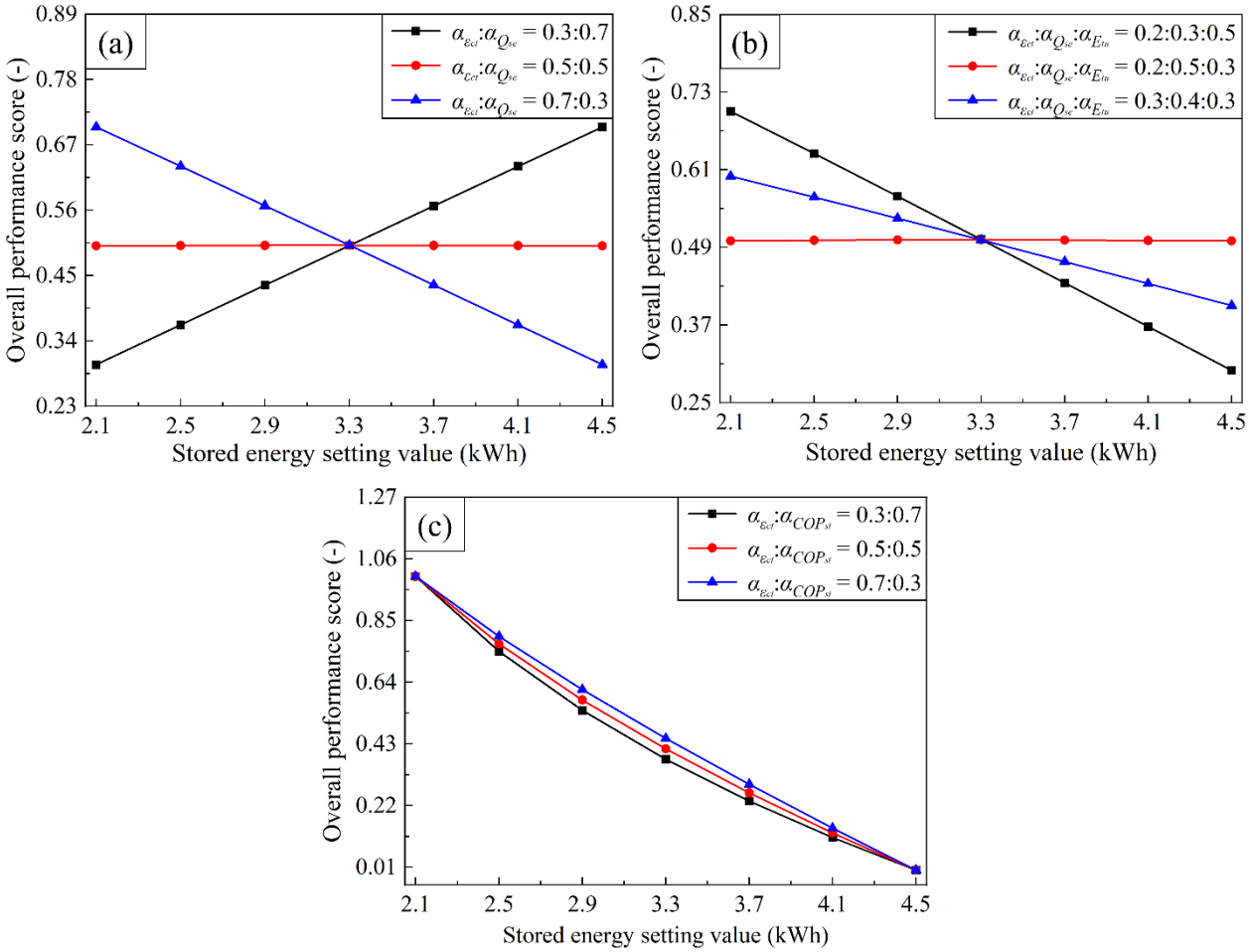

Fig. 4. (a) OS_{cs}, (b) OS_{cst}, and (c) OS_{cp} in different $Q_{se,sv}$ when ACHP is utilized

Fig. 5 depicts the variations of ε_{ct}, Q_{se}, E_{tu}, and COP_{st} with $Q_{se,sv}$ when WCHP is utilized. In Fig. 5(a), ε_{ct} linearly increased as $Q_{se,sv}$ increased. This implies that more time is required to complete the charging process to satisfy higher energy demands. As shown in Fig. 5(b), Q_{se} increased linearly with an increase in $Q_{se,sv}$. The Q_{se} values were almost identical to those of $Q_{se,sv}$, indicating that the Q-charging standard was successfully achieved. As shown in Fig. 5(c), E_{tu} increased linearly with $Q_{se,sv}$. This means that more electricity is required to satisfy higher energy demands. As shown in Fig. 5(d), COP_{st} decreases as $Q_{se,sv}$ increases. According to Eq. (3), this phenomenon implies that the degree of increase in Q_{se} with $Q_{se,sv}$ is smaller than that of E_{tu} with $Q_{se,sv}$. For instance, Q_{se} was 2.1 kWh and 2.5 kWh when $Q_{se,sv}$ was 2.1 kWh and 2.5 kWh, respectively. E_{tu} was 0.63 kWh and 0.76 kWh when $Q_{se,sv}$ was 2.1 kWh and 2.5 kWh, respectively. Thus, when $Q_{se,sv}$ increased from 2.1 kWh to 2.5 kWh, Q_{se} and E_{tu} increased by 19% and 22.1%,

respectively. This indicates that the increasing degree of Q_{se} with $Q_{se,sv}$ is smaller than that of E_{tu} with $Q_{se,sv}$. According to Eq. (3), COP_{st} was 3.36 and 3.27 when $Q_{se,sv}$ was 2.1 kWh and 2.5 kWh, respectively. Thus, the phenomenon of the increasing degree of Q_{se} with $Q_{se,sv}$ was smaller than that of E_{tu} with $Q_{se,sv}$ caused that COP_{st} reduced as $Q_{se,sv}$ increased.

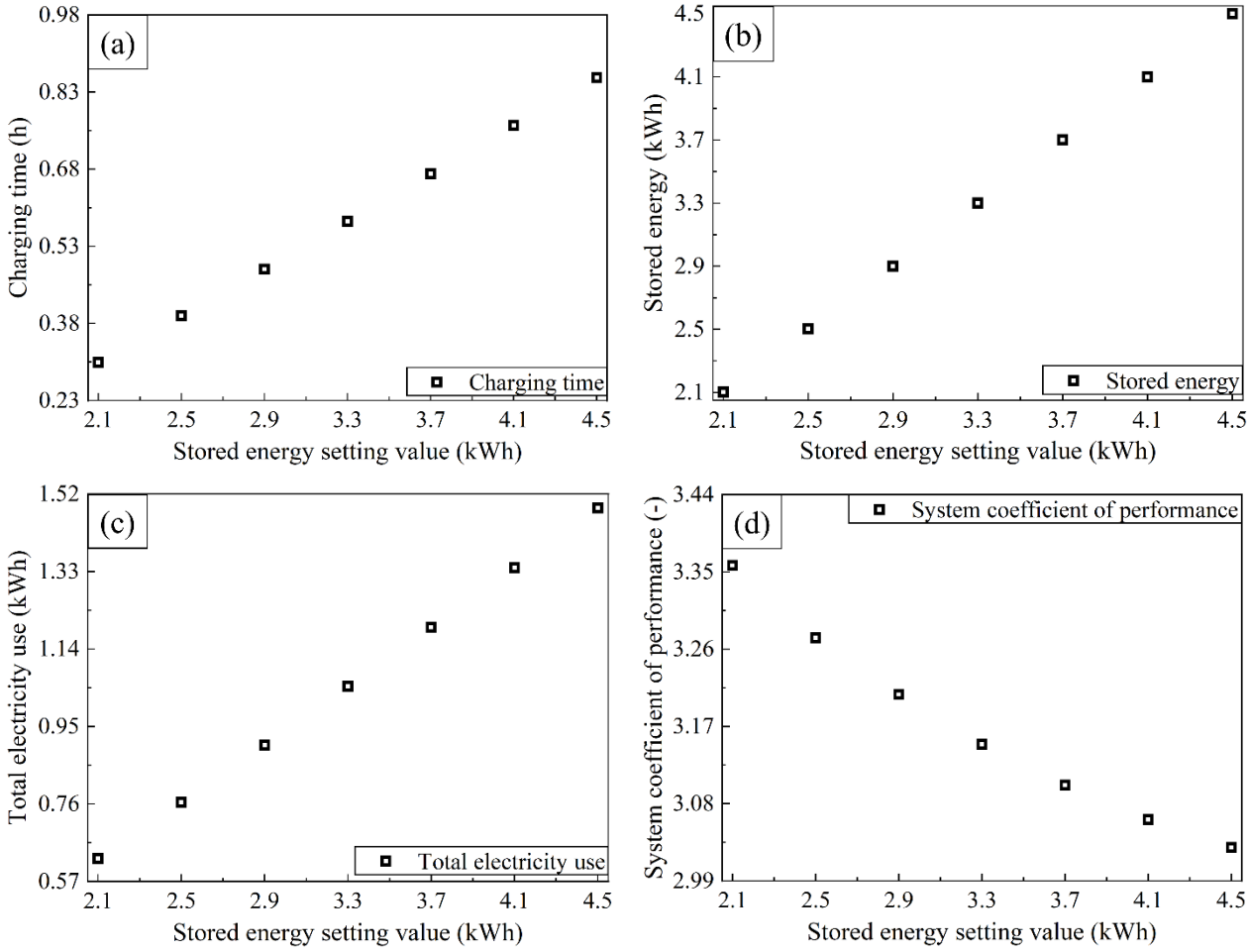

Fig. 5. (a) ε_{ct}, (b) Q_{se}, (c) E_{tu}, and (d) COP_{st} in different $Q_{se,sv}$ when WCHP is utilized

Fig. 6 depicts the variations in OS_{cs}, OS_{cst}, and OS_{cp} with $Q_{se,sv}$ when the WCHP system is utilized. In Fig. 6(a), the optimal $Q_{se,sv}$ were 4.5 kWh and 2.1 kWh in situations when $\alpha_{\varepsilon_{ct}}$:$\alpha_{Q_{se}}$ were 0.3:0.7 and 0.7:0.3, respectively. Although in the situation when $\alpha_{\varepsilon_{ct}}$:$\alpha_{Q_{se}}$ was 0.5:0.5, the variation of OS_{cs} with $Q_{se,sv}$ was small; the optimal $Q_{se,sv}$ was 2.9 kWh. Thus, larger $\alpha_{\varepsilon_{ct}}$ might cause the optimal $Q_{se,sv}$ to occur at a lower value. In Fig. 6(b), the optimal $Q_{se,sv}$ was 2.1 kWh in situations when $\alpha_{\varepsilon_{ct}}$:$\alpha_{Q_{se}}$:$\alpha_{E_{tu}}$ was 0.2:0.3:0.5 and 0.3:0.4:0.3. Although when $\alpha_{\varepsilon_{ct}}$:$\alpha_{Q_{se}}$:$\alpha_{E_{tu}}$

was 0.2:0.5:0.3, the variation of OS_{cst} with $Q_{se,sv}$ was small. The optimal $Q_{se,sv}$ was 2.9 kWh. Thus, the smaller $\alpha_{Q_{se}}$ would cause the optimal $Q_{se,sv}$ to occur at the lower value. In Fig. 6(c), the optimal $Q_{se,sv}$ is 2.1 kWh irrespective of $\alpha_{\varepsilon_{ct}}$:$\alpha_{COP_{st}}$ being 0.3:0.7, 0.5:0.5, or 0.7:0.3. Thus, regardless of whether ε_{ct} had a larger or smaller weighting than COP_{st}, the optimal $Q_{se,sv}$ occurred at a lower value.

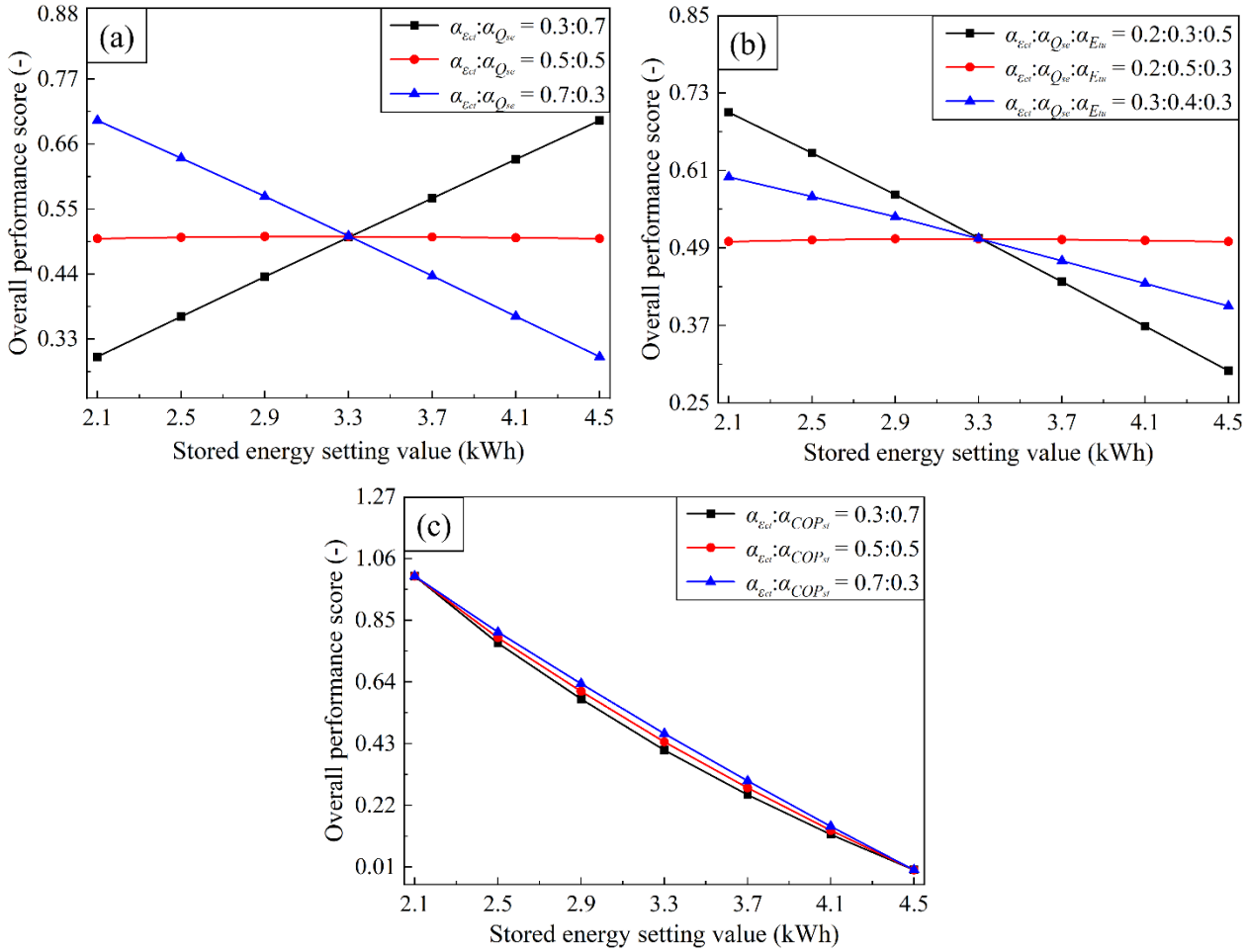

Fig. 6. (a) OS_{cs}, (b) OS_{cst}, and (c) OS_{cp} in different $Q_{se,sv}$ when WCHP is utilized

For the ACHP, ε_{ct}, Q_{se}, and E_{tu} increased by 126.1%, 114.2%, and 139.3%, respectively, when $Q_{se,sv}$ increased from 2.1 kWh to 4.5 kWh. COP_{st} was reduced by 10.5% when $Q_{se,sv}$ increased from 2.1 kWh to 4.5 kWh. For the WCHP, ε_{ct}, Q_{se}, and E_{tu} increased by 181.8%, 114.2%, and 137.5%, respectively, when $Q_{se,sv}$ increased from 2.1 kWh to 4.5 kWh. COP_{st} was reduced by 9.8% when $Q_{se,sv}$ increased from 2.1 kWh to 4.5 kWh. For ACHP and WCHP, in the multi-criteria

optimization considering ε_{ct} and Q_{se}, the effect of $\alpha_{\varepsilon_{ct}}$ on the optimal $Q_{se,sv}$ was almost the same as that of $\alpha_{Q_{se}}$ on the optimal $Q_{se,sv}$. In the multi-criteria optimization considering ε_{ct}, Q_{se}, and E_{tu}, the effect of $\alpha_{Q_{se}}$ on the optimal $Q_{se,sv}$ was larger than that of $\alpha_{\varepsilon_{ct}}$ and $\alpha_{E_{tu}}$ on the optimal $Q_{se,sv}$. In the multi-criteria optimization considering ε_{ct} and COP_{st}, the optimal $Q_{se,sv}$ was not affected by $\alpha_{Q_{se}}$ and $\alpha_{COP_{st}}$.

4.2. Results and discussion in the T-charging standard

In this section, we analyze the effects of $T_{ot,sv}$ on ε_{ct}, Q_{se}, E_{tu}, and COP_{st} in the T-charging standard. Fig. 7 depicts the variations of ε_{ct}, Q_{se}, E_{tu}, and COP_{st} with $T_{ot,sv}$ when ACHP was utilized. In Fig. 7(a), ε_{ct} increased as $T_{ot,sv}$ increased. This implies that more time is required to complete the charging process to satisfy the higher outlet water temperature demands. As shown in Fig. 7(b), Q_{se} increased as $T_{ot,sv}$ increased. As shown in Fig. 7(c), E_{tu} increases as $T_{ot,sv}$ increases. This means that more electricity is required to satisfy the higher outlet water temperature demands. As shown in Fig. 7 (d), COP_{st} reduced as $T_{ot,sv}$ increased. According to Eq. (3), this phenomenon implies that the degree of increase in Q_{se} with $T_{ot,sv}$ is smaller than that of E_{tu} with $T_{ot,sv}$. For instance, Q_{se} was 2.2 kWh and 2.5 kWh when $T_{ot,sv}$ was 28 °C and 29 °C, respectively. E_{tu} was 0.76 kWh and 0.88 kWh when $T_{ot,sv}$ was 28 °C and 29 °C, respectively. Thus, when $T_{ot,sv}$ increased from 28 °C to 29 °C, Q_{se} and E_{tu} increased by 13.3% and 15.8%, respectively. This indicates that the increasing degree of Q_{se} with $T_{ot,sv}$ is smaller than that of E_{tu} with $T_{ot,sv}$. According to Eq. (3), COP_{st} was 2.97 and 2.9 when $T_{ot,sv}$ was 28 °C and 29 °C, respectively. Thus, the phenomenon of the increasing degree of Q_{se} with $T_{ot,sv}$ was smaller than that of E_{tu} with $T_{ot,sv}$ caused that COP_{st} reduced as $T_{ot,sv}$ increased.

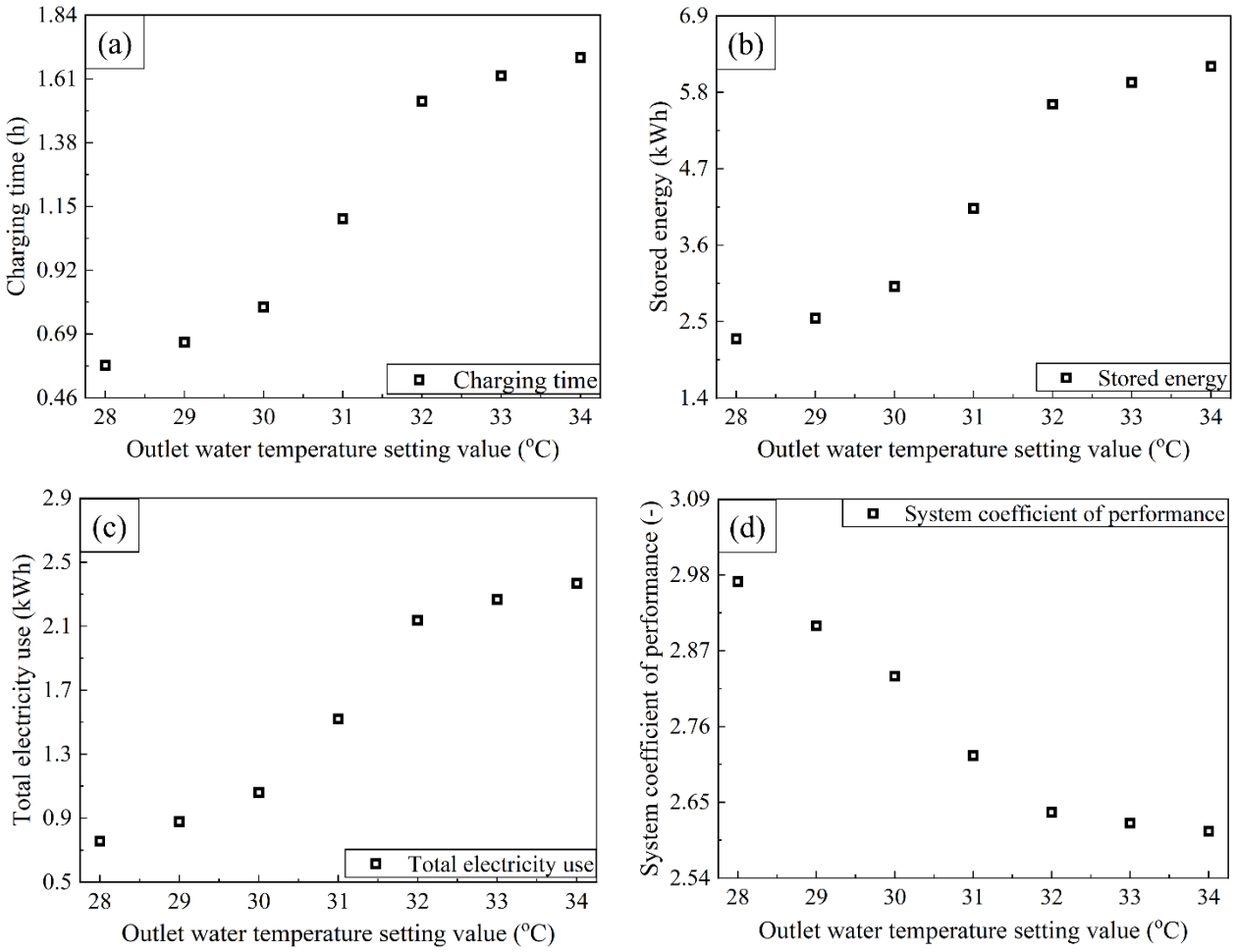

Fig. 7. (a) ε_{ct}, (b) Q_{se}, (c) E_{tu}, and (d) COP_{st} in different $T_{ot,sv}$ when ACHP is utilized

Fig. 8 shows the variations in OS_{cs}, OS_{cst}, and OS_{cp} with $T_{ot,sv}$ when the WCHP system was utilized. In Fig. 8(a), the optimal $T_{ot,sv}$ values were 34 °C and 28 °C when $\alpha_{\varepsilon_{ct}}$:$\alpha_{Q_{se}}$ were 0.3:0.7 and 0.7:0.3, respectively. When $\alpha_{\varepsilon_{ct}}$:$\alpha_{Q_{se}}$ was 0.5:0.5, the variation of OS_{cs} with $T_{ot,sv}$ was small; the optimal $T_{ot,sv}$ was 31 °C. Thus, the larger $\alpha_{\varepsilon_{ct}}$ might cause the optimal $T_{ot,sv}$ to occur at a lower value. In Fig. 8(b), the optimal $T_{ot,sv}$ was 28 °C when $\alpha_{\varepsilon_{ct}}$:$\alpha_{Q_{se}}$:$\alpha_{E_{tu}}$ was 0.2:0.3:0.5 and 0.3:0.4:0.3. When $\alpha_{\varepsilon_{ct}}$:$\alpha_{Q_{se}}$:$\alpha_{E_{tu}}$ was 0.2:0.5:0.3, the variation of OS_{cst} with $T_{ot,sv}$ was small; the optimal $T_{ot,sv}$ was 31 °C. Thus, it seemed that the smaller $\alpha_{Q_{se}}$ would cause the optimal $T_{ot,sv}$ to occur at a lower value. In Fig. 8(c), the optimal $T_{ot,sv}$ was 28 °C irrespective of $\alpha_{\varepsilon_{ct}}$:$\alpha_{COP_{st}}$ being 0.3:0.7, 0.5:0.5, or 0.7:0.3. Thus, regardless of whether ε_{ct} had a higher or lower weight than COP_{st}, the optimal $T_{ot,sv}$ had a lower value.

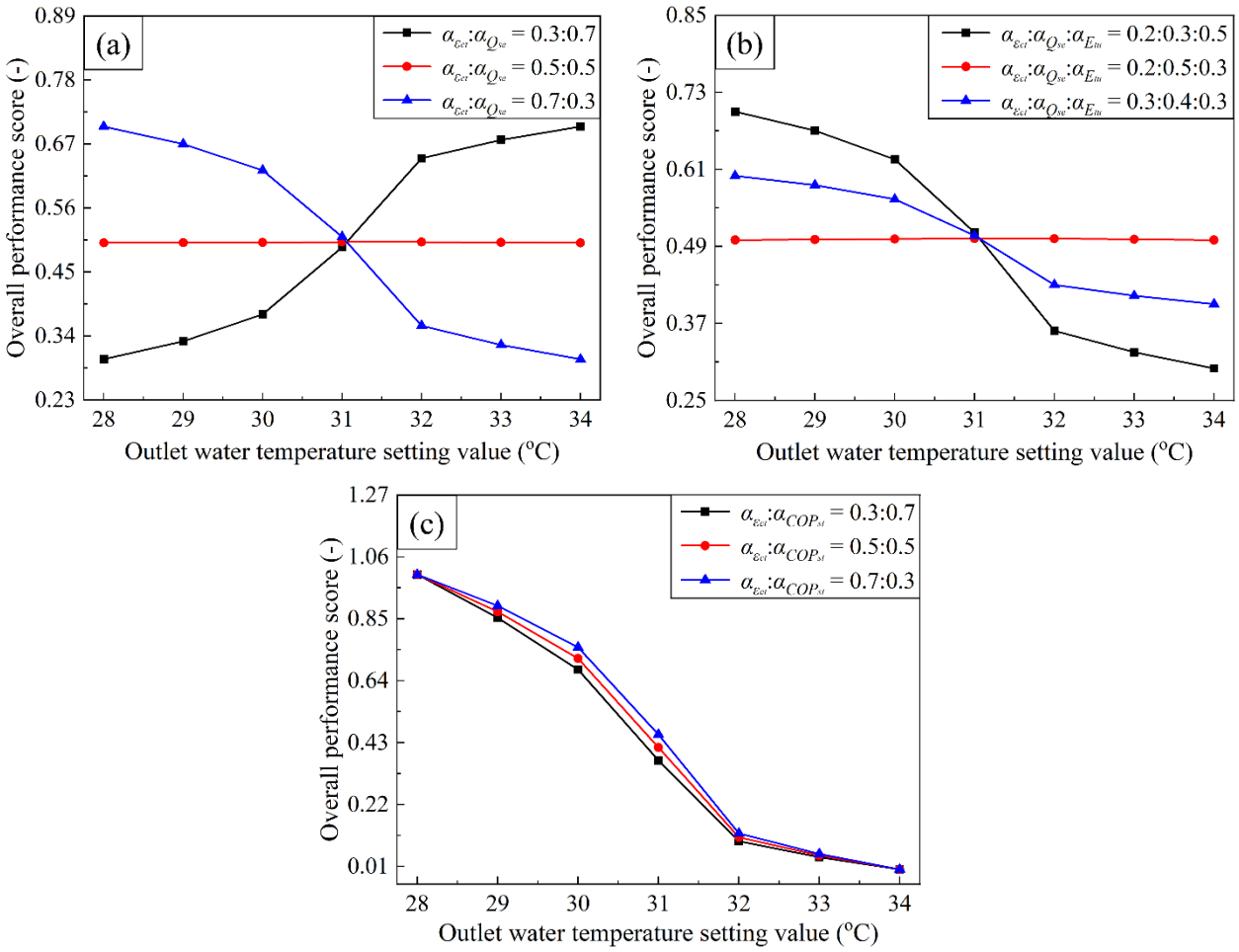

Fig. 8. (a) OS_{cs}, (b) OS_{cst}, and (c) OS_{cp} in different $T_{ot,sv}$ when ACHP is utilized

In previous studies [2], T-charging standard was not considered, and $T_{ot,sv}$ was fixed at 30 °C. In Fig. 8(a), when $\alpha_{\varepsilon_{ct}}:\alpha_{Q_{se}}$ was 0.3:0.7, OS_{cs} was 46.1% smaller when $T_{ot,sv}$ was 30 °C than that at 34 °C. When $\alpha_{\varepsilon_{ct}}:\alpha_{Q_{se}}$ was 0.7:0.3, OS_{cs} was 10.8% smaller when $T_{ot,sv}$ was 30 °C than that at 28 °C. In Fig. 8(b), when $\alpha_{\varepsilon_{ct}}:\alpha_{Q_{se}}:\alpha_{E_{tu}}$ was 0.2:0.5:0.3 and 0.3:0.4:0.3, the respective OS_{cs} values were 10.6% and 6.1% smaller when $T_{ot,sv}$ was 30 °C than that at 28 °C. In Fig. 8(c), when $\alpha_{\varepsilon_{ct}}:\alpha_{Q_{se}}$ were 0.3:0.7, 0.5:0.5, and 0.7:0.3, OS_{cs} values were 32.2%, 28.4%, and 24.7% smaller when $T_{ot,sv}$ was 30 °C than that at 28 °C, respectively.

Fig. 9 depicts the variations of ε_{ct}, Q_{se}, E_{tu}, and COP_{st} with $T_{ot,sv}$ when WCHP was utilized. In Fig. 9(a), ε_{ct} increased as $T_{ot,sv}$ increased. This implies that more time is required to complete the charging process to satisfy the higher outlet water temperature demands. As shown in Fig. 9(b),

Q_{se} increased as $T_{ot,sv}$ increased. As shown in Fig. 9(c), E_{tu} increases as $T_{ot,sv}$ increases. This means that more electricity is required to satisfy the higher outlet water temperature demands. As shown in Fig. 9(d), COP_{st} reduced as $T_{ot,sv}$ increased. According to Eq. (3), this phenomenon implies that the degree of increase in Q_{se} with $T_{ot,sv}$ is smaller than that of E_{tu} with $T_{ot,sv}$. For instance, Q_{se} was 2.1 kWh and 2.2 kWh when $T_{ot,sv}$ was 28 °C and 29 °C, respectively. E_{tu} was 0.63 kWh and 0.66 kWh when $T_{ot,sv}$ was 28 °C and 29 °C, respectively. Thus, when $T_{ot,sv}$ increased from 28 °C to 29 °C, Q_{se} and E_{tu} increased by 4% and 4.6%, respectively. This indicates that the increasing degree of Q_{se} with $T_{ot,sv}$ is smaller than that of E_{tu} with $T_{ot,sv}$. According to Eq. (3), COP_{st} was 3.35 and 3.34 when $T_{ot,sv}$ was 28 °C and 29 °C, respectively. Thus, the phenomenon of the increasing degree of Q_{se} with $T_{ot,sv}$ was smaller than that of E_{tu} with $T_{ot,sv}$ caused that COP_{st} reduced as $T_{ot,sv}$ increased.

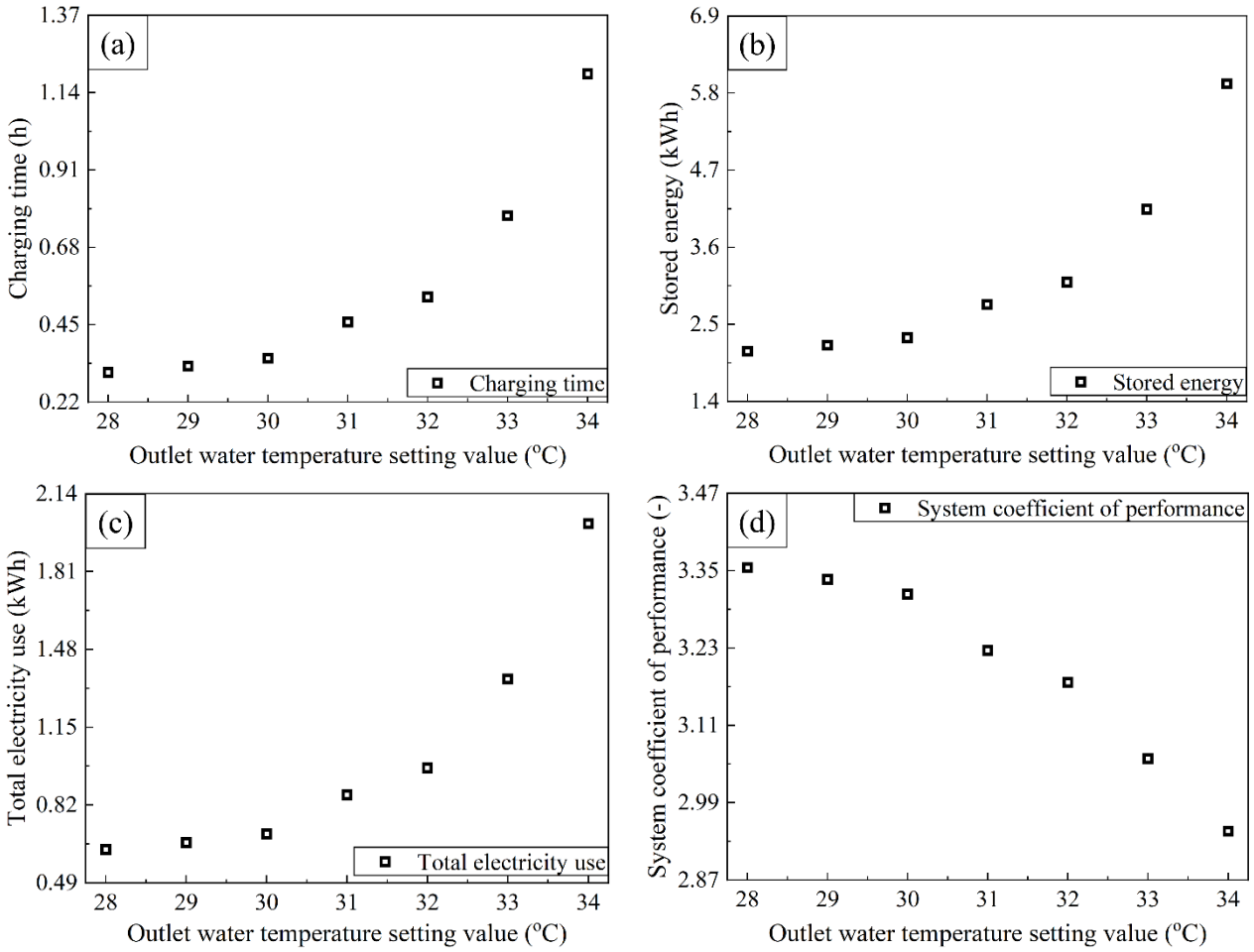

Fig. 9. (a) ε_{ct}, (b) Q_{se}, (c) E_{tu}, and (d) COP_{st} in different $T_{ot,sv}$ when WCHP is utilized

Fig. 10 shows the variations in OS_{cs}, OS_{cst}, and OS_{cp} with $T_{ot,sv}$ when the WCHP system was utilized. In Fig. 10(a), the optimal $T_{ot,sv}$ were 34 °C and 28 °C when $\alpha_{\varepsilon_{ct}}$:$\alpha_{Q_{se}}$ were 0.3:0.7 and 0.7:0.3, respectively. When $\alpha_{\varepsilon_{ct}}$:$\alpha_{Q_{se}}$ was 0.5:0.5, the variation of OS_{cs} with $T_{ot,sv}$ was small; the optimal $T_{ot,sv}$ was 32 °C. Thus, the larger $\alpha_{\varepsilon_{ct}}$ might cause the optimal $T_{ot,sv}$ to occur at a lower value. In Fig. 10(b), the optimal $T_{ot,sv}$ was 28 °C when $\alpha_{\varepsilon_{ct}}$:$\alpha_{Q_{se}}$:$\alpha_{E_{tu}}$ was 0.2:0.3:0.5 and 0.3:0.4:0.3. When $\alpha_{\varepsilon_{ct}}$:$\alpha_{Q_{se}}$:$\alpha_{E_{tu}}$ was 0.2:0.5:0.3, the variation of OS_{cst} with $T_{ot,sv}$ was small; the optimal $T_{ot,sv}$ was 32 °C. Thus, it seemed that the smaller $\alpha_{Q_{se}}$ would cause the optimal $T_{ot,sv}$ to occur at the lower value. In Fig. 10(c), the optimal $T_{ot,sv}$ was 28 °C irrespective of $\alpha_{\varepsilon_{ct}}$:$\alpha_{COP_{st}}$ being 0.3:0.7, 0.5:0.5, or 0.7:0.3. Thus, regardless of whether ε_{ct} had a larger or smaller weighting than COP_{st}, the optimal $T_{ot,sv}$ occurred at a lower value.

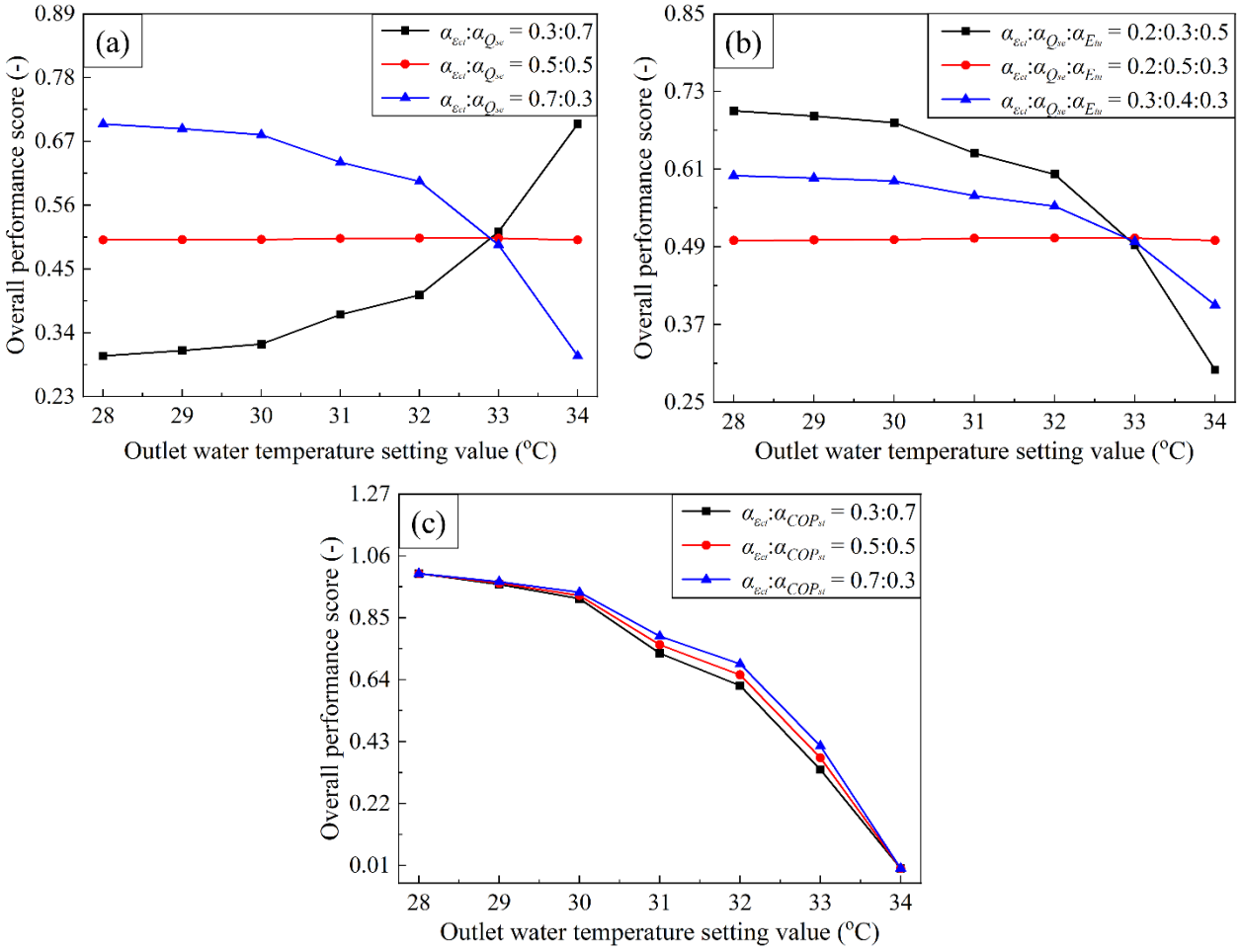

Fig. 10. (a) OS_{cs}, (b) OS_{cst}, and (c) OS_{cp} in different $T_{ot,sv}$ when WCHP is utilized

In previous studies [2], T-charging standard was not considered, and $T_{ot,sv}$ was fixed at 30 °C. In Fig. 10(a), when $\alpha_{\varepsilon_{ct}}$: $\alpha_{Q_{se}}$ was 0.3:0.7, OS_{cs} was 54.2% smaller when $T_{ot,sv}$ was 30 °C than that at 34 °C. When $\alpha_{\varepsilon_{ct}}$: $\alpha_{Q_{se}}$ was 0.7:0.3, OS_{cs} was 2.7% smaller when $T_{ot,sv}$ was 30°C than that at 28 °C. In Fig. 10(b), when $\alpha_{\varepsilon_{ct}}$: $\alpha_{Q_{se}}$: $\alpha_{E_{tu}}$ was 0.2:0.5:0.3 and 0.3:0.4:0.3, the respective OS_{cs} values were 2.6% and 1.4% when $T_{ot,sv}$ was 30 °C than that at 28 °C, respectively. In Fig. 10(c), when $\alpha_{\varepsilon_{ct}}$: $\alpha_{Q_{se}}$ were 0.3:0.7, 0.5:0.5, and 0.7:0.3, OS_{cs} values were 8.5%, 7.4%, and 6.4% smaller when $T_{ot,sv}$ was 30 °C than that at 28 °C, respectively.

For the ACHP, ε_{ct}, Q_{se}, and E_{tu} increased by 192.5%, 174.4%, and 212.5%, respectively, when $T_{ot,sv}$ increased from 28 °C to 34 °C. COP_{st} was reduced by 12.2% when $T_{ot,sv}$ increased from 28 °C to 34 °C. For the WCHP, ε_{ct}, Q_{se}, and E_{tu} increased by 288.2%, 180.2%, and 219.1% when $T_{ot,sv}$ increased from 28 °C to 34 °C. COP_{st} was reduced by 12.2% when $T_{ot,sv}$ increased from 28 °C to 34 °C. For ACHP and WCHP, in the multi-criteria optimization considering ε_{ct} and Q_{se}, the effect of $\alpha_{\varepsilon_{ct}}$ on the optimal $T_{ot,sv}$ was almost the same as that of $\alpha_{Q_{se}}$ on the optimal $T_{ot,sv}$. In the multi-criteria optimization considering ε_{ct}, Q_{se}, and E_{tu}, the effect of $\alpha_{Q_{se}}$ on the optimal $T_{ot,sv}$ was larger than that of $\alpha_{\varepsilon_{ct}}$ and $\alpha_{E_{tu}}$ on the optimal $T_{ot,sv}$. In the multi-criteria optimization considering ε_{ct} and COP_{st}, the optimal $T_{ot,sv}$ was not affected by $\alpha_{Q_{se}}$ and $\alpha_{COP_{st}}$.

4.3. Results and discussion in the t-charging standard

In this section, we analyze the effects of $\varepsilon_{ct,sv}$ on ε_{ct}, Q_{se}, E_{tu}, and COP_{st} in the t-charging standard. Fig. 11 depicts the variations of ε_{ct}, Q_{se}, E_{tu}, and COP_{st} with $\varepsilon_{ct,sv}$ when ACHP is utilized. In Fig. 11 (a), ε_{ct} linearly increased with the increase of $\varepsilon_{ct,sv}$. The ε_{ct} values were almost the same as those of $\varepsilon_{ct,sv}$. This means that the t-charging standard was successfully achieved. In Fig. 11(b), Q_{se} linearly increased with the increase of $\varepsilon_{ct,sv}$. This meant that more energy would be stored if ε_{ct} was longer. In Fig. 11(c), E_{tu} linearly increased with the increase of $\varepsilon_{ct,sv}$. This meant that more electricity would be utilized if ε_{ct} was longer. In Fig. 11(d), COP_{st} reduced as $\varepsilon_{ct,sv}$ increased. According to Eq. (3), this phenomenon implies that the degree of increase in Q_{se} with $\varepsilon_{ct,sv}$ is smaller than that of E_{tu} with $\varepsilon_{ct,sv}$. For instance, Q_{se} was 2 kWh and 2.7 kWh when $\varepsilon_{ct,sv}$ was 0.5 h and 0.7 h, respectively. E_{tu} was 0.65 kWh and 0.93 kWh when $\varepsilon_{ct,sv}$ was 0.5 h and 0.7 h, respectively. Thus, when $\varepsilon_{ct,sv}$ increased from 0.5 h to 0.7 h, Q_{se} and E_{tu} increased by 36.2%

and 43.9%, respectively. This indicates that the increasing degree of Q_{se} with $\varepsilon_{ct,sv}$ is smaller than that of E_{tu} with $\varepsilon_{ct,sv}$. According to Eq. (3), COP_{st} was 3.04 and 2.88 when $\varepsilon_{ct,sv}$ was 0.5 h and 0.7 h, respectively. Thus, the phenomenon of the increasing degree of Q_{se} with $\varepsilon_{ct,sv}$ was smaller than that of E_{tu} with $\varepsilon_{ct,sv}$ caused that COP_{st} reduced as $\varepsilon_{ct,sv}$ increased.

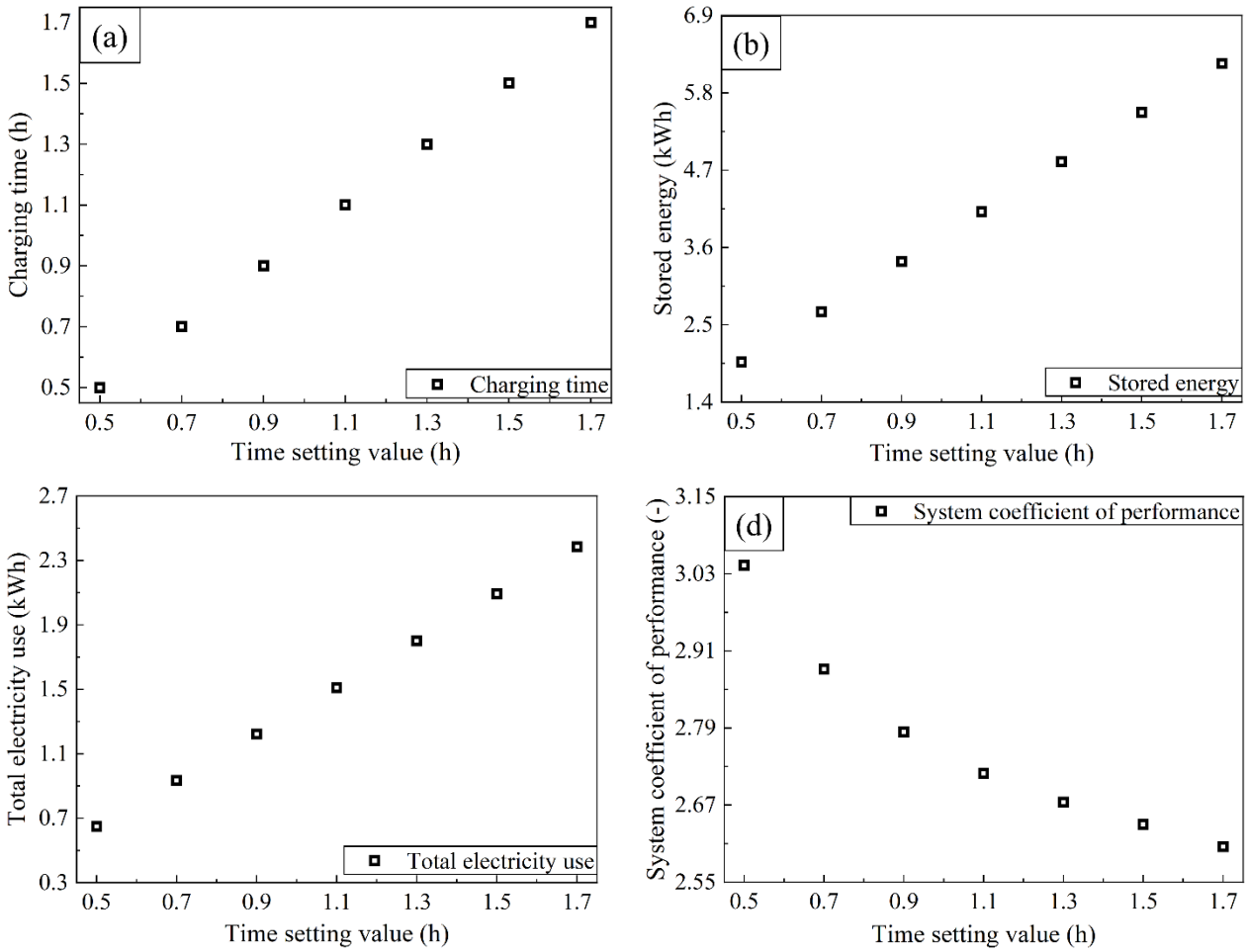

Fig. 11. (a) ε_{ct}, (b) Q_{se}, (c) E_{tu}, and (d) COP_{st} in different $\varepsilon_{ct,sv}$ when ACHP is utilized

Fig. 12 depicts the variations of OS_{cs}, OS_{cst}, and OS_{cp} with $\varepsilon_{ct,sv}$ when ACHP is utilized. In Fig. 12(a), the optimal $\varepsilon_{ct,sv}$ were 1.7 h and 0.5 h when $\alpha_{\varepsilon_{ct}}$: $\alpha_{Q_{se}}$ were 0.3:0.7 and 0.7:0.3, respectively. When $\alpha_{\varepsilon_{ct}}$: $\alpha_{Q_{se}}$ was 0.5:0.5, the variation of OS_{cs} with $\varepsilon_{ct,sv}$ was small; the optimal $\varepsilon_{ct,sv}$ was 1.3 h. Thus, the larger $\alpha_{\varepsilon_{ct}}$ might cause the optimal $\varepsilon_{ct,sv}$ to occur at the lower value. In Fig. 12(b), the optimal $\varepsilon_{ct,sv}$ was 0.5 h when $\alpha_{\varepsilon_{ct}}$: $\alpha_{Q_{se}}$: $\alpha_{E_{tu}}$ was 0.2:0.3:0.5 and 0.3:0.4:0.3. When $\alpha_{\varepsilon_{ct}}$: $\alpha_{Q_{se}}$: $\alpha_{E_{tu}}$ was 0.2:0.5:0.3, the variation of OS_{cst} with $\varepsilon_{ct,sv}$ was small; the optimal $\varepsilon_{ct,sv}$ was

1.1 h. Thus, it seemed that the smaller $\alpha_{Q_{se}}$ would cause the optimal $\varepsilon_{ct,sv}$ to occur at the lower value. In Fig. 12(c), the optimal $\varepsilon_{ct,sv}$ is 0.5 h irrespective of $\alpha_{\varepsilon_{ct}}$: $\alpha_{COP_{st}}$ being 0.3:0.7, 0.5:0.5, or 0.7:0.3. Thus, regardless of whether ε_{ct} had a larger or smaller weighting than COP_{st}, the optimal $\varepsilon_{ct,sv}$ occurred at a lower value.

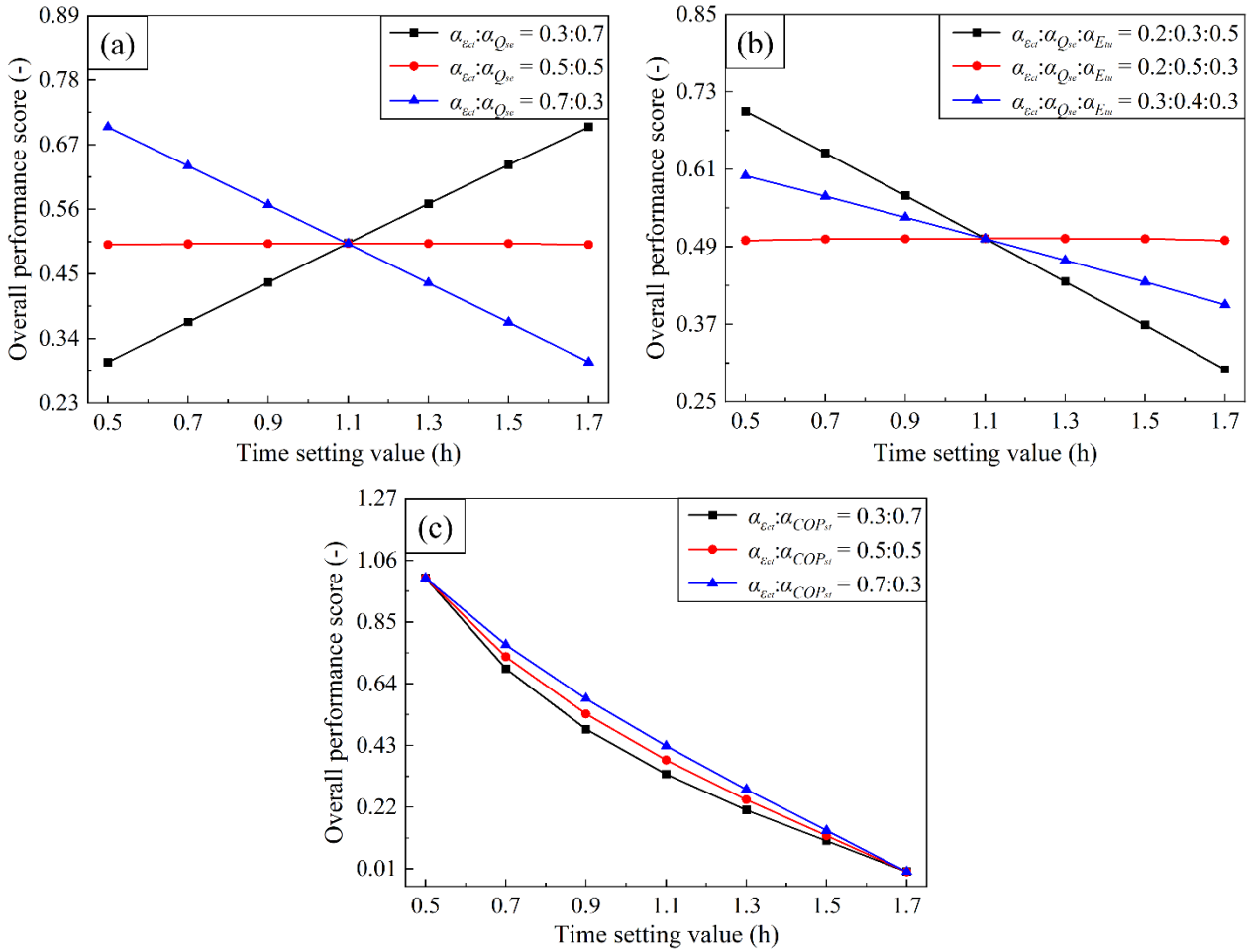

Fig. 12. (a) OS_{cs}, (b) OS_{cst}, and (c) OS_{cp} in different $\varepsilon_{ct,sv}$ when ACHP is utilized

Fig. 13 depicts the variations of ε_{ct}, Q_{se}, E_{tu}, and COP_{st} with $\varepsilon_{ct,sv}$ when WCHP is utilized. In Fig. 13(a), ε_{ct} linearly increased with the increase of $\varepsilon_{ct,sv}$. The ε_{ct} values were almost the same as those of $\varepsilon_{ct,sv}$. This meant that the t-charging standard was successfully achieved. In Fig. 13(b), Q_{se} linearly increased as $\varepsilon_{ct,sv}$ increased. This meant that more energy would be stored if ε_{ct} was longer. In Fig. 13(c), E_{tu} linearly increased as $\varepsilon_{ct,sv}$ increased. This meant that more electricity would be utilized if ε_{ct} was longer. In Fig. 13(d), COP_{st} reduced as $\varepsilon_{ct,sv}$ increased.

According to Eq. (3), this phenomenon implies that the degree of increase in Q_{se} with $\varepsilon_{ct,sv}$ is smaller than that of E_{tu} with $\varepsilon_{ct,sv}$. For instance, Q_{se} was 3 kWh and 3.8 kWh when $\varepsilon_{ct,sv}$ was 0.5 h and 0.7 h, respectively. E_{tu} was 0.93 kWh and 1.2 kWh when $\varepsilon_{ct,sv}$ was 0.5 h and 0.7 h, respectively. Thus, when $\varepsilon_{ct,sv}$ increased from 0.5 h to 0.7 h, Q_{se} and E_{tu} increased by 29% and 33.6%, respectively. This indicates that the increasing degree of Q_{se} with $\varepsilon_{ct,sv}$ is smaller than that of E_{tu} with $\varepsilon_{ct,sv}$. According to Eq. (3), COP_{st} was 3.2 and 3.09 when $\varepsilon_{ct,sv}$ was 0.5 h and 0.7 h, respectively. Thus, the phenomenon of the increasing degree of Q_{se} with $\varepsilon_{ct,sv}$ was smaller than that of E_{tu} with $\varepsilon_{ct,sv}$ caused that COP_{st} reduced as $\varepsilon_{ct,sv}$ increased.

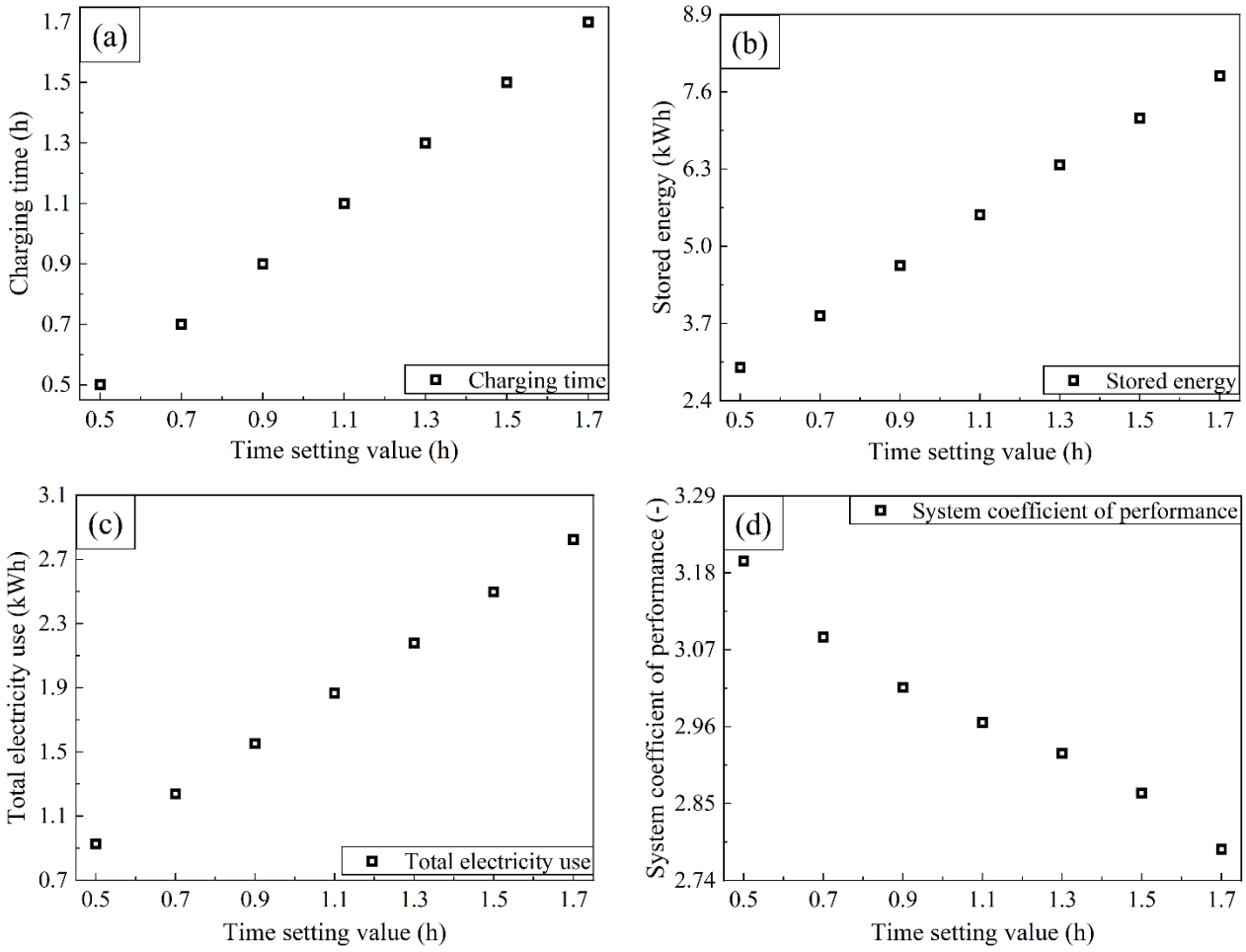

Fig. 13. (a) ε_{ct}, (b) Q_{se}, (c) E_{tu}, and (d) COP_{st} in different $\varepsilon_{ct,sv}$ when WCHP is utilized

Fig. 14 depicts the variations of OS_{cs}, OS_{cst}, and OS_{cp} with $\varepsilon_{ct,sv}$ when WCHP is utilized. In Fig. 14(a), the optimal $\varepsilon_{ct,sv}$ were 1.7 h and 0.5 h when $\alpha_{\varepsilon_{ct}}$: $\alpha_{Q_{se}}$ were 0.3:0.7 and 0.7:0.3, respectively.

When $\alpha_{\varepsilon_{ct}}$:$\alpha_{Q_{se}}$ was 0.5:0.5, the variation of OS_{cs} with $\varepsilon_{ct,sv}$ was small. The optimal $\varepsilon_{ct,sv}$ was 1.3 h. Thus, the larger $\alpha_{\varepsilon_{ct}}$ might cause the optimal $\varepsilon_{ct,sv}$ to occur at the lower value. In Fig. 14(b), the optimal $\varepsilon_{ct,sv}$ was 0.5 h when $\alpha_{\varepsilon_{ct}}$:$\alpha_{Q_{se}}$:$\alpha_{E_{tu}}$ was 0.2:0.3:0.5 and 0.3:0.4:0.3. When $\alpha_{\varepsilon_{ct}}$:$\alpha_{Q_{se}}$:$\alpha_{E_{tu}}$ was 0.2:0.5:0.3, the variation of OS_{cst} with $\varepsilon_{ct,sv}$ was small; the optimal $\varepsilon_{ct,sv}$ was 1.3 h. Thus, it seemed that the smaller $\alpha_{Q_{se}}$ would cause the optimal $\varepsilon_{ct,sv}$ to occur at the lower value. In Fig. 14(c), the optimal $\varepsilon_{ct,sv}$ was 0.5 h irrespective of the situation when $\alpha_{\varepsilon_{ct}}$:$\alpha_{COP_{st}}$ was 0.3:0.7, 0.5:0.5, or 0.7:0.3. Thus, regardless of whether ε_{ct} had a larger or smaller weighting than COP_{st}, the optimal $\varepsilon_{ct,sv}$ occurred at a lower value.

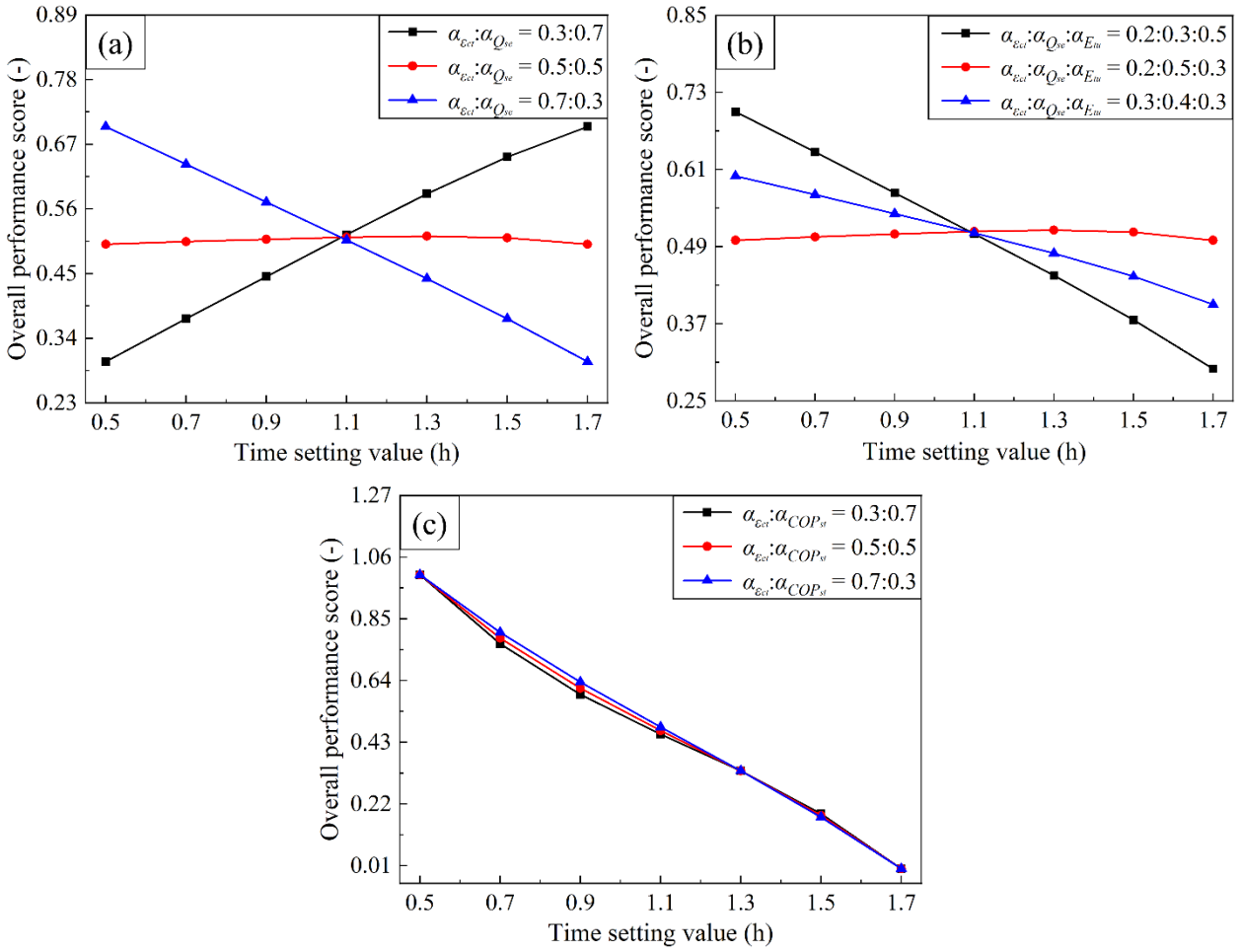

Fig. 14. (a) OS_{cs}, (b) OS_{cst}, and (c) OS_{cp} in different $\varepsilon_{ct,sv}$ when WCHP is utilized

For the ACHP, ε_{ct}, Q_{se}, and E_{tu} increased by 240%, 214.9%, and 267.7%, respectively, when $\varepsilon_{ct,sv}$ increased from 0.5 h to 1.7 h. COP_{st} was reduced by 14.4% when $\varepsilon_{ct,sv}$ increased from 0.5 h

to 1.7 h. For the WCHP, ε_{ct}, Q_{se}, and E_{tu} increased by 240%, 165.2%, and 204.5%, respectively, when $\varepsilon_{ct,sv}$ increased from 0.5 h to 1.7 h. COP_{st} was reduced by 12.9% when $\varepsilon_{ct,sv}$ increased from 0.5 h to 1.7 h. For ACHP and WCHP, in the multi-criteria optimization considering ε_{ct} and Q_{se}, the effect of $\alpha_{\varepsilon_{ct}}$ on the optimal $\varepsilon_{ct,sv}$ was almost the same as that of $\alpha_{Q_{se}}$ on the optimal $\varepsilon_{ct,sv}$. In the multi-criteria optimization considering ε_{ct}, Q_{se}, and E_{tu}, the effect of $\alpha_{Q_{se}}$ on the optimal $\varepsilon_{ct,sv}$ was larger than that of $\alpha_{\varepsilon_{ct}}$ and $\alpha_{E_{tu}}$ on the optimal $\varepsilon_{ct,sv}$. In the multi-criteria optimization considering ε_{ct} and COP_{st}, the optimal $\varepsilon_{ct,sv}$ was not affected by $\alpha_{Q_{se}}$ and $\alpha_{COP_{st}}$.

5. Conclusions

To illustrate the influence of charging standards and combinations of setting variables on the performance of the closed-loop charging system, a system integrating CO_2 heat pumps and a PCM tank was investigated. Furthermore, ACHP and WCHP were considered. The system was simulated using an experimentally validated CO_2 heat pump and PCM tank model. The effects of $T_{ot,sv}$, $Q_{se,sv}$, and ε_{ct} on the performance of the system in the T-charging, Q-charging, and t-charging standards were analyzed, respectively. We found that for ACHP, COP_{st} was reduced by 10.5% when $Q_{se,sv}$ increased from 2.1 kWh to 4.5 kWh. COP_{st} reduced by 12.2% when $T_{ot,sv}$ increased from 28 °C to 34 °C. COP_{st} reduced by 14.4% when $\varepsilon_{ct,sv}$ increased from 0.5 h to 1.7 h. For WCHP, COP_{st} reduced by 9.8% when $Q_{se,sv}$ increased from 2.1 kWh to 4.5 kWh. COP_{st} reduced by 12.2% when $T_{ot,sv}$ increased from 28 °C to 34 °C. COP_{st} reduced by 12.9% when $\varepsilon_{ct,sv}$ increased from 0.5 h to 1.7 h.

Additionally, the multi-criteria optimization was performed in three cases where the combinations of ε_{ct} and Q_{se}, ε_{ct}, E_{tu}, and Q_{se}, and ε_{ct} and COP_{st} were considered. The optimal $T_{ot,sv}$, $Q_{se,sv}$, and $\varepsilon_{ct,sv}$ were identified in the T-charging, Q-charging, and t-charging standards, respectively. We concluded that for ACHP and WCHP, in the multi-criteria optimization considering ε_{ct} and Q_{se}, the effect of $\alpha_{\varepsilon_{ct}}$ on the optimal $\varepsilon_{ct,sv}$ was almost the same as that of $\alpha_{Q_{se}}$ on the optimal $\varepsilon_{ct,sv}$. In the multi-criteria optimization considering ε_{ct}, Q_{se}, and E_{tu}, the effect of $\alpha_{Q_{se}}$ on the optimal $\varepsilon_{ct,sv}$ was larger than that of $\alpha_{\varepsilon_{ct}}$ and $\alpha_{E_{tu}}$ on the optimal $\varepsilon_{ct,sv}$. In the multi-criteria optimization considering ε_{ct} and COP_{st}, the optimal $\varepsilon_{ct,sv}$ was not affected by $\alpha_{Q_{se}}$ and $\alpha_{COP_{st}}$. Hence, this study provides a different perspective for investigating a system with an integrated heat pump and

PCM tank by considering different charging standards and multiple criteria.

6. Future works

The limitations of this study and corresponding future developments are summarized below. First, the physical characteristics of the ground-source CO_2 heat pump differed from those of ACHP and WCHP systems. Therefore, a system integrating a ground-source CO_2 heat pump with a PCM tank should be investigated. The influence of tube diameter, borehole depth, and diameter on ε_{ct}, Q_{se}, E_{tu}, and COP_{st} in different charging standards should be analyzed in the future. Second, the PCM tank was assumed to have no heat exchange with the ambient environment. The heat loss coefficient of the PCM tank may affect the optimization results when a multi-criteria approach was applied. The influence of the PCM tank heat-loss coefficient on the system performance under different charging standards should be considered in the future. Finally, the surrogate models for describing relationships between ε_{ct} and setting variables and between COP_{st} and setting variables contribute to identifying optimal setting variables more accurately. Reliable surrogate models should be developed using advanced methods, such as machine learning, in the future.

Acknowledgements

This work is supported by Guangdong Basic and Applied Basic Research Foundation (2022A1515140105) and Guangdong Provincial University Youth Innovative Talent Project (2024KQNCX154). This work is supported by Guangdong Provincial University Innovation Team Project, No. 2023KCXTD038. This project has received funding from the European Union's Horizon 2020 research and innovation programme under the Marie Skłodowska-Curie grant agreement No [895732]. This publication has been jointly written within the cooperative project "Key technologies and demonstration of combined cooling, heating and power generation for low-carbon neighbourhoods/buildings with clean energy – ChiNoZEN". The authors gratefully acknowledge the funding support from the Research Council of Norway (NRC project number 304191 - ENERGIX) and from the Ministry of Science and Technology of China (MOST project number 2019YFE0104900).

References

[1] T. Zhang, F. Wang, Y. Gao, Y. Liu, Q. Guo, Q. Zhao, Optimization of a solar-air source heat pump system in the high-cold and high-altitude area of China, Energy 268 (2023).

[2] Y. Li, N. Nord, H. Yin, An investigation of using CO_2 heat pumps to charge PCM storage tank for domestic use, Renewable Energy 218 (2023).

[3] P. Mi, J. Zhang, J. Gao, Y. Han, Study on optimal allocation of solar photovoltaic thermal heat pump integrated energy system for domestic hot water, Renewable Energy 219 (2023).

[4] Y. Hou, W. Wu, Z. Li, X. Yu, T. Zeng, Effect of drying air supply temperature and internal heat exchanger on performance of a novel closed-loop transcritical CO_2 air source heat pump drying system, Renewable Energy 219 (2023).

[5] W. Liu, J. Yao, T. Jia, Y. Zhao, Y. Dai, J. Zhu, V. Novakovic, The performance optimization of DX-PVT heat pump system for residential heating, Renewable Energy 206 (2023) 1106-1119.

[6] A. Pesola, Cost-optimization model to design and operate hybrid heating systems – Case study of district heating system with decentralized heat pumps in Finland, Energy 281 (2023).

[7] N.H. Petersen, M. Arras, M. Wirsum, L. Ma, Integration of large-scale heat pumps to assist sustainable water desalination and district cooling, Energy 289 (2024).

[8] Z. Tan, X. Feng, M. Yang, Y. Wang, Energy and economic performance comparison of heat pump and power cycle in low grade waste heat recovery, Energy 260 (2022).

[9] Z. Shao, Z.G. Wang, P. Poredoš, T.S. Ge, R.Z. Wang, Highly efficient desiccant-coated heat exchanger-based heat pump to decarbonize rail transportation, Energy 271 (2023).

[10] N. Zhang, Y. Lu, Z.H. Ouderji, Z. Yu, Review of heat pump integrated energy systems for future zero-emission vehicles, Energy 273 (2023).

[11] X. Liu, Y. Hu, Q. Wang, L. Yao, M. Li, Energetic, environmental and economic comparative analyses of modified transcritical CO2 heat pump system to replace R134a system for home heating, Energy 229 (2021).

[12] Ç. Yıldız, M. Seçilmiş, M. Arıcı, M.S. Mert, S. Nižetić, H. Karabay, An experimental study on a solar-assisted heat pump incorporated with PCM based thermal energy storage unit, Energy 278 (2023).

[13] Q. Al-Yasiri, M. Szabó, Experimental study of PCM-enhanced building envelope towards energy-saving and decarbonisation in a severe hot climate, Energy and Buildings 279 (2023).

[14] T. Xiong, H.W. Kua, K.W. Shah, G.F. Hussein, B. Zhang, Graphene nanoplatelets and copper foams for improving passive cooling performance of PCMs in Singapore's tropical climate, Journal of Energy Storage 80 (2024).
[15] K. Zhang, C. Hu, H. Huang, B. Li, C. Huang, S. Wang, Achieving efficient energy utilization by PCM in the food supply chain: Encapsulation technologies, current applications, and future prospects, Journal of Energy Storage 79 (2024).
[16] M. Elsayed, M. Salah Mansour, M.A. Eid, M.M. Abdel-Raouf, Thermal behavior of frozen products paired with PCM during winter and summer power outages, Case Studies in Thermal Engineering 53 (2024).
[17] S. Jalilian, M. Momeni, A. Fartaj, Enhancing thermal performance and optimization strategies of PCM-integrated slab-finned two-fluid heat exchangers for sustainable thermal management, Journal of Energy Storage 75 (2024).
[18] A. Chibani, S. Merouani, H. Laidoudi, A. Dehane, L. Bendada, L. Lamiri, G. Mecheri, C. Bougriou, N. Gherraf, Numerical simulation and analysis of heat transfer and melting rate of nano-enhanced PCM composite embedded in a concentrator photovoltaic system, Journal of Energy Storage 73 (2023).
[19] E. Assareh, A. Riaz, M. Ahmadinejad, S. Hoseinzadeh, M.Z. Abdehvand, S. Keykhah, T. Jafarinejad, R. Moltames, M. Lee, Enhancing solar thermal collector systems for hot water production through machine learning-driven multi-objective optimization with phase change material (PCM), Journal of Energy Storage 73 (2023).
[20] M. E.A.E. Ahmed, S. Abdo, M.A. Abdelrahman, O.A. Gaheen, Finned-encapsulated PCM pyramid solar still – Experimental study with economic analysis, Journal of Energy Storage 73 (2023).
[21] Y. Wang, Z. Quan, Y. Zhao, L. Wang, Z. Bai, J. Shi, Energy and exergy analysis of a novel dual-source heat pump system with integrated phase change energy storage, Renewable Energy (2023).
[22] B. Du, Z. Quan, L. Hou, Y. Zhao, X. Lou, S. Shao, Simulation analysis of a photovoltaic/thermal-air dual heat source direct-expansion heat pump, Renewable Energy 218 (2023).

[23] H.H. Shin, K. Kim, M. Lee, C. Han, Y. Kim, Maximized thermal energy utilization of surface water-source heat pumps using heat source compensation strategies under low water temperature conditions, Energy 288 (2024).
[24] S. Zhang, S. Liu, J. Wang, Y. Li, Z. Yu, Analysis of a solar-assisted heat pump system with hybrid energy storage for space heating, Applied Thermal Engineering 231 (2023).
[25] J. Deng, Y. Su, C. Peng, W. Qiang, W. Cai, Q. Wei, H. Zhang, How to improve the energy performance of mid-deep geothermal heat pump systems: Optimization of heat pump, system configuration and control strategy, Energy 285 (2023).
[26] T.S. Ge, Z.C. Weng, R. Huang, B. Hu, T.M. Eikevik, Y.J. Dai, High temperature transcritical CO2 heat pump with optimized tube-in-tube heat exchanger, Energy 283 (2023).
[27] Y. Li, N. Nord, H. Halvorsen, I. Håvard Rekstad, Model-based sizing of a CO_2 heat pump for residential use, Sustainable Energy Technologies and Assessments 53 (2022).
[28] T.A. Sazon, H. Nikpey, Modeling and investigation of the performance of a solar-assisted ground-coupled CO2 heat pump for space and water heating, Applied Thermal Engineering 236 (2024).
[29] W.M. Duarte, S.N. Rabelo, T.F. Paulino, J.J.G. Pabón, L. Machado, Experimental performance analysis of a CO_2 direct-expansion solar assisted heat pump water heater, International Journal of Refrigeration 125 (2021) 52-63.
[30] E. Zanetti, S. Bordignon, R. Conte, A. Bisi, M. Azzolin, A. Zarrella, Experimental and numerical analysis of a CO2 dual-source heat pump with PVT evaporators for residential heating applications, Applied Thermal Engineering 233 (2023).
[31] S. Huang, W. Li, J. Lu, Y. Li, Z. Wang, S. Zhu, Experimental study on thermal performances of a solar chimney with and without PCM under different system inclination angles, Energy 290 (2024).
[32] Z. Guermat, Y. Kabar, F. Kuznik, T.E. Boukelia, Numerical investigation of the integration of new bio-based PCM in building envelopes during the summer in Algerian cities, Journal of Energy Storage 79 (2024).
[33] A. Khan, N. Shahzad, A. Waqas, M. Mahmood, M. Ali, S. Umar, Unlocking the potential of passive cooling: A comprehensive experimental study of PV/PCM/TEC hybrid system for enhanced photovoltaic performance, Journal of Energy Storage 80 (2024).

[34] H.M. Maghrabie, A.S.A. Mohamed, A.M. Fahmy, A.A. Abdel Samee, Performance enhancement of PV panels using phase change material (PCM): An experimental implementation, Case Studies in Thermal Engineering 42 (2023).
[35] X. Zheng, Z. Tang, Y. Wang, H. Liu, Performance of the air source heat pump assisted solar heating system combined with PCM floor, Applied Thermal Engineering 239 (2024).
[36] D. Qv, L. Ni, Y. Yao, W. Hu, Reliability verification of a solar–air source heat pump system with PCM energy storage in operating strategy transition, Renewable Energy 84 (2015) 46-55.
[37] D. Zou, X. Ma, X. Liu, P. Zheng, B. Cai, J. Huang, J. Guo, M. Liu, Experimental research of an air-source heat pump water heater using water-PCM for heat storage, Applied Energy 206 (2017) 784-792.
[38] J.-Y. Long, D.-S. Zhu, Numerical and experimental study on heat pump water heater with PCM for thermal storage, Energy and Buildings 40(4) (2008) 666-672.
[39] P. Moreno, A. Castell, C. Solé, G. Zsembinszki, L.F. Cabeza, PCM thermal energy storage tanks in heat pump system for space cooling, Energy and Buildings 82 (2014) 399-405.
[40] M. Qiu, B. Peng, X. Xu, Y. Zhou, R. Zhang, F. Su, J. Xin, Synergistic impact of horizontal fin installation height and nanoparticle volume fraction to enhance charging performance of phase change materials (PCMs), International Communications in Heat and Mass Transfer 154 (2024).
[41] O.O. Issa, V. Thirunavukkarasu, Experimental study on charging and discharging behavior of PCM encapsulations for thermal energy storage of concentrating solar power system, Journal of Energy Storage 85 (2024).
[42] B. Peng, M. Qiu, N. Xu, Y. Zhou, W. Sheng, F. Su, Optimum orthogonally structured fins in charging enhancement of phase change materials (PCMs): PCMs' thermophysical properties effects, International Journal of Thermal Sciences 184 (2023).
[43] G. Shu, T. Xiao, J. Guo, P. Wei, X. Yang, Y.-L. He, Effect of charging/discharging temperatures upon melting and solidification of PCM-metal foam composite in a heat storage tube, International Journal of Heat and Mass Transfer 201 (2023).
[44] B.P. Rasmussen, A.G. Alleyne, Dynamic modeling and advanced control of air conditioning and refrigeration systems, Air Conditioning and Refrigeration Center. College of Engineering …, 2006.

692 [45] Y. Li, G. Huang, H. Wu, T. Xu, Feasibility study of a PCM storage tank integrated heating
693 system for outdoor swimming pools during the winter season, Applied Thermal Engineering 134
694 (2018) 490-500.
695 [46] W. Deng, J. Yu, Simulation analysis on dynamic performance of a combined solar/air dual
696 source heat pump water heater, Energy Conversion and Management 120 (2016) 378-387.
697 [47] E. Lee, H. Kang, Y. Kim, Flow boiling heat transfer and pressure drop of water in a plate heat
698 exchanger with corrugated channels at low mass flux conditions, International Journal of Heat and
699 Mass Transfer 77 (2014) 37-45.
700 [48] F.A. Mota, E. Carvalho, M.A. Ravagnani, Modeling and Design of Plate Heat Exchanger,
701 Heat Transfer: Studies and Applications (2015) 165.
702 [49] S. Wang, H. Tuo, F. Cao, Z. Xing, Experimental investigation on air-source transcritical CO_2
703 heat pump water heater system at a fixed water inlet temperature, International Journal of
704 Refrigeration 36(3) (2013) 701-716.
705 [50] I.W. Eames, A. Milazzo, G.G. Maidment, Modelling thermostatic expansion valves,
706 International Journal of Refrigeration 38 (2014) 189-197.
707 [51] T. Watanabe, H. Kikuchi, A. Kanzawa, Enhancement of charging and discharging rates in a
708 latent heat storage system by use of PCM with different melting temperatures, Heat Recovery
709 Systems and CHP 13(1) (1993) 57-66.
710 [52] Y. Li, N. Zhang, Z. Ding, Investigation on the energy performance of using air-source heat
711 pump to charge PCM storage tank, Journal of Energy Storage 28 (2020).
712 [53] Y. Li, Z. Ding, M. Shakerin, N. Zhang, A multi-objective optimal design method for thermal
713 energy storage systems with PCM: A case study for outdoor swimming pool heating application,
714 Journal of Energy Storage 29 (2020).
715 [54] Y. Li, N. Nord, H. Wu, Z. Yu, G. Huang, A study on the integration of air-source heat pumps,
716 solar collectors, and PCM tanks for outdoor swimming pools for winter application in subtropical
717 climates, Journal of Building Performance Simulation 13(6) (2020) 662-683.

718